NTNU
Norwegian University of
Science and Technology

Model of single-phase synchronous machine for rotary frequency converter

Developement of time-domain model,
including excitation system

Erik Johan Jenssen

Master of Energy and Environmental Engineering
Submission date: June 2016
Supervisor: Trond Toftevaag, ELKRAFT

Norwegian University of Science and Technology
Department of Electric Power Engineering

Preface

This is a Master's thesis written on behalf of NTNU as a part of the study program, Master of Science in Energy and Environmental Engineering. It was carried out during the spring semester of 2016, initiated in January and ended in June. The thesis is written in collaboration with Jernbaneverket (The Norwegian National Rail Administration). Jernbaneverket came up with the idea of the project, and after an inquiry, I was fortunate to be assigned to this project.

Trondheim, 2016-06-23

Erik Johan Jenssen

Acknowledgment

The process of writing this thesis has been hard and challenging with moments of frustration. In such moments I was fortunate to get support from people around me.

Particularly, I would like to thank my supervisor Trond Toftevaag (Associate Professor) at the Department of Electric Power Engineering. He has been enthusiastic about the topic and has been given me valuable guidance through the whole work process, and has been a great source of motivation.

I would also like to thank Dr. Steinar Danielsen at Jernbaneverket, which came up with the project and has provided me with vital help and information.

Furthermore, I would like to thank Prof. Arnd Stephan and Dipl.-Ing. Christoph Pache at TU Dresden, for answering my emails and providing me with helpful information.

And lastly, I would like to thank my family and friends for all your support and encouragement.

E.J.J.

Problem description

- Developement of a mathematical model of a single-phase synchronous machine in the time domain, including exciter and voltage regulator
- The model is to be implemented in a suitable modelling software tool e.g. MATLAB/Simulink, Simpow or similar.
- The model is meant to represent a part of a rotary frequency converter, that is used in the norwegian traction power system.
- The model shall be verified through simulations and comparative analysis (if time permits).

Summary

This thesis concerns the development of a single-phase synchronous machine model in time-domain, with instantaneous value output. The model is meant to represent the generator part of the rotary converter used in the Norwegian traction power system (supplying railway). Its function is to convert the 50 Hz frequency of the main grid into 16 $\frac{2}{3}$ Hz, which is the standard frequency of the traction grid in Norway.

The chosen method of modelling is inspired by previous work on this matter. The solution is to model the single-phase machine by using a standard three-phase machine model, with unsymmetrical loading on two of its phases. The third phase is left idle. The equations of the standard synchronous machine model are used.

An adjustment of the parameters is questioned, followed by a suggested set of parameter values on the basis of analysis and mathematical deduction.

A comparative approach is used in the validation of the model. Jernbaneverket has done some measurements of the actual rotary converter, which have been compared to simulations of the model.

According to these comparisons, the model has proven to reflect the general behavior of the rotary converter. High correlation can be achieved by adjusting the parameters. Nevertheless, no conclusion has been made upon the adjustment of the parameters.

Sammendrag

Jernbanens roterende frekvensomformere består av to synkronmaskiner, en trefasemaskin og en enfasemaskin koblet på samme rotoraksling. Frekvensomformerens hovedoppgave er å forsyne jernbanenettet med 16 2/3 Hz, via regionalnettet. Per idag mangler Jernbaneverket en momentanverdimodell av enfasemaskinen i denne omformeren. Denne masteroppgaven omhandler utvikling av nevnte modell.

I arbeidet med å lage modellen er det hentet inspirasjon fra andre lignende publikasjoner. Enfasemaskinen er modellert ved å benytte en standard trefasemaskin som er belastet over to faser, der den siste fasen er ute av drift. Dermed kan likningene til standardmodellen tas i bruk.

Det er diskutert hvorvidt om parameterne må endres i en slik modell, som har resultert i noen endringsforslag.

Validering av modellen er gjort ved hjelp av komparativ analyse. Simulerte utfall er sammenlignet med målinger mottatt av Jernbaneverket.

Simuleringene har vist seg å korrelere med målingene til en viss grad. Svært høy korrelasjon kan oppnås ved å justere på parameterne. Det er ikke gjort noen konklusjoner i parameterjusteringen.

Contents

Chapter 1

Introduction

1.1 Background

Länderbahnen (The German State railways) signed in 1912 an agreement setting standards for the traction power system. The voltage standard was decided to be $15kV$ AC single-phase with a frequency of $16\frac{2}{3}Hz$. Prior this year, most of the locomotives run on direct-current propulsion, with power being supplied via an overhead contact line. Due to practical reasons, it was desired to change to an AC standard. The low $16\frac{2}{3}Hz$ frequency was necessary for operating the series-wound commutator motors, in order to achieve sparkless commutation and reduced heating of magnetic components (due to eddy currents). This standard was adopted by Austria, Sweden, Switzerland and Norway.

In Norway, the traction power system is fed by two general types of converters; static and dynamic converters. The majority is supplied by dynamic converters, which are the old type of converters (some machines have been in service for more than 50 years). The static converters are based on power electronics, and will eventually replace the dynamic converters.

The dynamic converters are also known as rotary converters, which consists of two synchronous machines coupled together, where one of them is connected to the main grid, and the other to the traction power system. The main purpose of the converters is to transform the main power grid frequency (50Hz) into the traction power grid frequency ($16\frac{2}{3}Hz$). This is accomplished by having a three-to-one ratio on the machine rotor poles, such that the main grid machine has three times more poles than the traction machine. The machine on the traction power grid side is mainly operated as a generator, while the machine on the main grid side is mainly operating as a motor. A reversed direction of power may be accomplished if the train is in a regenerative breaking mode of operation.

Even though these rotary converters are old, they represent 70-80% of the traction power supply, and will be in operation for many years ahead. It is therefore of importance to study how these converters interact with the traction power grid, the main power grid, the locomotives and the overall stability. This creates a need for modelling the system to predict these interactions, simulation of fault cases and for stability analysis.

Engineers in Jernbaneverket (The Norwegian National Rail Administration) have created a model of these converters, connected in a network similar to the real traction power network. This model has been used for analytical studies, concerning stability and testing of new components or new locomotives. Although, it is lacking the instantaneous value model. Instantaneous value models of three-phase synchronous machines exists, but the single-phase machine model is missing. The development of such a model will therefore be the main objective in this master thesis.

1.2 Problem description and objectives

The main objectives of this Master's project are

1. Developement of a mathematical model of a single-phase synchronous machine in the time domain, including exciter and voltage regulator
2. The model shall have the possibility of instantaneous value output
3. The model is to be implemented in a suitable modelling software tool e.g. MATLAB/Simulink, Simpow or similar.
4. The model shall be verified through simulations and comparative analysis (if time per-

mits).

The model is to be interconnected to a three-phase synchronous machine, and should be able to reproduce the characteristics of the rotary frequency converter. After completion of the model, simulations of the model is to be performed. The simulations should be based on a few cases in which measurements are available, so that comparisons can be made, and eventually ensure validation of the model.

1.3 Approach and method

The development of a mathematical model is comprehensive work. The work involved a lot of literature research, experimentation, trial and failure in own derivation and mathematical testing. The main approach chosen for the work in this thesis was to find a theoretical basis in literature that could constitute the starting point of the mathematical model.

Literature Survey

Single-phase synchronous machines are only used in special cases, such as traction power supply, and are not described in conventional electric machinery literature. It has therefore been a challenge finding proper literature on this narrow topic.

The most relevant findings were these:

- "Dynamisches Verhalten von Synchron-Synchron-Umformern" by Torsten Stoltze. The translated title is "Dynamic behavior of synchronous synchronous converters". This publication has been the major source of inspiration when it comes to modelling of the single-phase synchronous machine. Although, it is written in German and required translation.
- "Single-Phase Synchronous Machine" (1947) by I. A. Terry and B. L. Robertson . This is a quite old article, but it describes the theory of single-phase synchronous machines. The machines described are three-phase machines with unsymmetrical loading, similar to the approach in this thesis. The method of symmetrical components is used in the analysis.

Other relevant sources on the issue:

- "Electric Traction Stability" (2010) by Steinar Danielsen. This doctoral thesis has been the main source on everything that concerns the rotating converter and the traction network. Parameters and other details used in the model are fetched from this publication.
- "Power System Stability and Control" (1994) by Prabha Kundur. This book is giving a profound description of synchronous machines, parameters and control.
- "Power System Dynamics: Stability and Control" (2008) by Jan Machowski. This a book that presents many details of the synchronous machines, with better explanation than other literature on the matter.

1.3.1 Work process

The preliminary state of the work process consisted of a general literature survey, where the first read was the PhD thesis of Dr. Steinar Danielsen. This gave a good introduction to the rotary converter and its dynamics. Thereafter, a study of synchronous machines was carried out.

The core of the problem was to find a way to model the single-phase synchronous machine, which seemed to be a non-existing topic in the literature. It was performed a comprehensive search for literature that could be of help in solving the problem.

After a while, a publication from TU Dresden by Torsten Stoltze appeared. This is written in German, and required translation. Despite the language barriers, the publication showed extreme relevance and presented an approach of modelling which is adopted in this thesis.

With this background it was possible to create an outline of the model.

Attempt to implement model in Simpow

Jernbaneverket requested an implementation of the model in the Simpow simulation software.

- Due to a lack of experience with DSL (dynamic simulation language) coding, it was decided to use the DSL code generator program, "HiDraw", for the implementation of the model. This is a block diagram drawing program that converts the diagram into DSL code which can be used in the Simpow software. The diagram was finished, and can be seen in appendix C. But the code did not compile, and moving on to write the code instead was recommended.

- Since the model is using the same equations as the standard model, the code for a standard model was obtained. After a while, as more concepts were understood, some of the code was developed (can be found in appendix D). Due to some errors and problems (singularity issue?) the code development was terminated.
- Since the writer is more experienced with the MATLAB/Simulink software tool, it was chosen as an alternative, which resulted in a successful implementation

1.4 Structure of the report

The rest of the report is structured as follows. Chapter 2 gives an introduction to the single-phase machine and its application in rotary frequency converters. Chapter 3 is presenting the mathematical model of the single-phase synchronous machines, both its electrical part and its mechanical part. The excitation system is also considered in this chapter.

Chapter 4 gives a description of the parameters of the machine, and a possible adjustment of the parameter values are suggested. In chapter 5, one can find a presentation of how the model is implemented in a dynamic simulation software tool.

Chapter 6 deals with simulations, results and discussion. And at the end, the conclusive part is found in chapter 7.

Chapter 2

Single-Phase Machines and Rotating Frequency Converters

This chapter will give a short introduction to how the single-phase machine is designed, some if its special features. The rotating frequency converter will also be described.

2.1 The design and features of single-phase synchronous machines

The low-frequency single-phase machines described in this thesis, are of salient-pole construction, having one sinusoidally distributed stator winding in the armature. The rotor is containing a field winding, which is supplied with a field current through the exciter. The rotating field will induce a current in the stator winding if the machine is in a generating mode of operation. Adjustment of the field voltage will indirectly control the stator voltage.

The magnetic field of a single-phase machine will not rotate as in a three-phase machine. The single-phase current is basically a sine wave pulsating at the line frequency from peak positive to peak negative, and the same applies to the magnetic field in the single-phase winding. While the three-phase machine has three such windings producing a field rotating in space, the single-phase machine has only one pulsating field directed either up or down. Because of this, one may interpret the pulsating field as two rotating components; one rotating on the forward direction and one in the backward direction. Together they produce the pulsating field. The rotor will obviously only follow one of these fields, preferably the forward direction field. The backward direction field component will in that case produce a undesirable current in the rotor (at twice the line frequency). Because of this, the rotor has to have a damper winding that is able to reduce the effect of the backward field component in the stator.

The pulsation of the magnetic field also applies to the power and torque. If the single-phase machine is in motoring mode, some oscillation may be observable in the rotor. In general, the pulsation is largely compensated by the rotational inertia. At standstill, there is no net torque, and the starting sequence is therefore requiring an external starting force. As soon as rotation is present, the machine will develop a rotating torque in the airgap.

The machine in question is the one found in the rotating frequency converters in the Norwegian traction system. The single-phase machine is generally operating as generator in this situation, as discussed in the next section.

2.2 The rotating frequency converter

The Norwegian traction power system is supplied mainly by rotary converters. These are of the type synchronous-synchronous, which implies one synchronous machine operating as a generator, driven by another synchronous machine operating as a motor. The motor is connected to the main 50 Hz grid, and is a standard three-phase machine. The generator is mechanically connected on the same rotor shaft, which is a single-phase synchronous machine and supplies the traction power grid at $16\frac{2}{3}Hz$. The frequency conversion is achieved by having a 3-to-1 ratio on the rotor poles of the machines, where the motor has 12 poles while the generator has 4 poles. Both machine has its own excitation system and AVR. Transformers are connected to the input and output terminals.

The rotary converters are stationed in pairs or more, and located along the railway lines, from

20 to 90 km apart. The converters considered are of the type ASEA Q38.

Chapter 3

The development of the mathematical model

The dynamic model of the three-phase synchronous machine is well established and is standardized in the "IEEE Standard 1110-2002" [15] . The single-phase model is not developed in the common literature, due to its rare usage. This chapter will first present the standard three-phase synchronous machine model, and thereafter the single phase model. All the equations in the synchronous machine model is based in the rotating reference frame (using dq-values). The dq-transformation will firstly be presented. All equations are written for per unit quantities.

Remark: The following representation of the single-phase synchronous machine is inspired by the derivation by Torsten Stoltze in [19]. This approach of modelling is acknowledged and verified by researchers from TU Dresden. A similar approach is described in [14].

3.1 The dq-transformation

The modelling of electrical machines is of simplicity reasons based in the direct and quadrature axis. The transformation is reducing the three AC quantities into two DC quantities, and is in this way reducing the amount of effort in further calculations. Robert H. Park developed this transformation in 1929, and is now the standard approach in the study of electrical machines. The transformations will be presented in the following.

3.1.1 From three-phase quantities to dq-quantities

$$\begin{bmatrix} S_\mathrm{d} \\ S_\mathrm{q} \\ S_0 \end{bmatrix} = \beta \begin{bmatrix} cos(\theta) & cos(\theta - \frac{2\pi}{3}) & cos(\theta + \frac{2\pi}{3}) \\ -sin(\theta) & -sin(\theta - \frac{2\pi}{3}) & -sin(\theta + \frac{2\pi}{3}) \\ \beta_0 & \beta_0 & \beta_0 \end{bmatrix} \begin{bmatrix} S_\mathrm{a} \\ S_\mathrm{b} \\ S_\mathrm{c} \end{bmatrix} \tag{3.1}$$

The variable S is representing the quantity being transformed, and can be currents, flux linkages or other quantities. The coefficient β may have two different values, both can be used for different reasons (as long as the same coefficient is used in the backward transformation):

- $\beta_{dq} = \frac{2}{3}$, $\beta_0 = \frac{1}{2}$
- $\beta_{dq}\sqrt{\frac{2}{3}}$, $\beta_0 = \frac{1}{\sqrt{2}}$

The choice of β is varying in literature. In this thesis, $\beta_{dq} = \frac{2}{3}$ is used for two reasons: (1) Simulink is using this coefficient in the model blocks. (2) The number of turns is a key point in the derivation in this thesis. "With a current transformation coefficient of 2/3 both the d- and q-axis armature coils have the same number of turns as an individual phase winding." [7]

The angle θ is the angle between the rotors direct axis and a fixed axis. The fixed axis is in most cases the a winding. With this, the three-phase quantities are now transformed to dq-quantities located in the rotating reference frame.

3.1.2 From dq-quantities to three-phase quantities

$$\begin{bmatrix} S_a \\ S_b \\ S_c \end{bmatrix} = \sqrt{\frac{2}{3}} \begin{bmatrix} cos(\theta) & -sin(\theta) & \frac{1}{\sqrt{2}} \\ cos(\theta - \frac{2\pi}{3}) & -sin(\theta - \frac{2\pi}{3}) & \frac{1}{\sqrt{2}} \\ cos(\theta + \frac{2\pi}{3}) & -sin(\theta + \frac{2\pi}{3}) & \frac{1}{\sqrt{2}} \end{bmatrix} \begin{bmatrix} S_a \\ S_b \\ S_c \end{bmatrix} \tag{3.2}$$

3.2 Modelling synchronous machines

The different ways of modelling synchronous machines are graded by the level of accuracy and complexity. IEEE has made a map of categories listed in the table below.

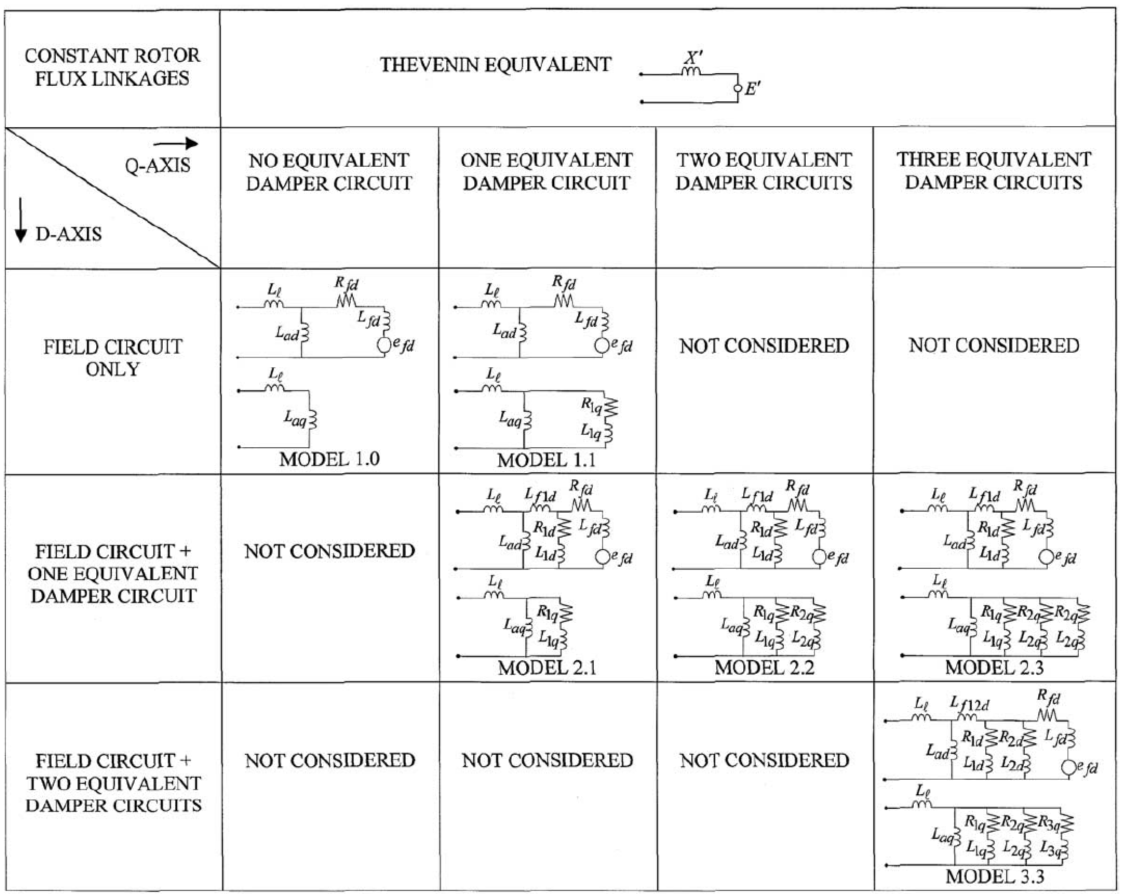

CONSTANT ROTOR FLUX LINKAGES	THEVENIN EQUIVALENT			
Q-AXIS → / D-AXIS ↓	NO EQUIVALENT DAMPER CIRCUIT	ONE EQUIVALENT DAMPER CIRCUIT	TWO EQUIVALENT DAMPER CIRCUITS	THREE EQUIVALENT DAMPER CIRCUITS
FIELD CIRCUIT ONLY	MODEL 1.0	MODEL 1.1	NOT CONSIDERED	NOT CONSIDERED
FIELD CIRCUIT + ONE EQUIVALENT DAMPER CIRCUIT	NOT CONSIDERED	MODEL 2.1	MODEL 2.2	MODEL 2.3
FIELD CIRCUIT + TWO EQUIVALENT DAMPER CIRCUITS	NOT CONSIDERED	NOT CONSIDERED	NOT CONSIDERED	MODEL 3.3

Figure 3.1: Selection of generator models of varying degrees of complexity from IEEE Std 1110

For the modelling in this paper, the model 2.1 has been chosen, which is also the one studied in the Stolze paper [19] . This model has one equivalent damper circuit in the d-axis and one in the q-axis. A more detailed model would require many more parameters than is available.

The standard 2.1 model will now be presented as it is, with a three-phase configuration. In order to model it as a single-phase machine, some adjustments will be made. These adjustments will be presented after.

3.3 The three-phase synchronous machine model in time domain

The following presentation will give a brief overview of the equations related to the model. This is the commonly accepted model of a salient-pole synchronous machine, and is the one found in *IEEE-1110-2002* [15]. All the equations are expressed in the dq-axis, whereas the phase values (a b c) can be calculated using the dq-transformation.

The equivalent dq-windings

The model has three sets of windings illustrated in Figure 3.2. The three sets are perpendicular to each other, and have therefore no magnetic coupling between each other. The d-winding represents the three-phase stator winding in the d-axis, while the D-winding represents the damper winding of the rotor. The f-winding corresponds to the field winding in the rotor.

The second set of windings are in the q-axis and consists of the q and the Q windings , which are the equivalents to the stator windings in the q-axis and the damper winding in the rotor q-axis.

The third set, the zero winding can be omitted because the stator windings are connected in star with the neutral point isolated.

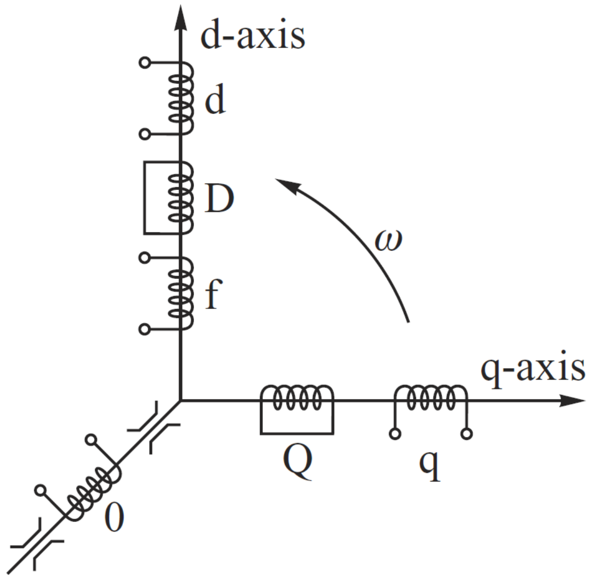

Figure 3.2: The equivalent dq-windings representing the synchronous machine

In this representation, the q-axis in lagging the d-axis. This is the reference basis used in Machowski [7]. Although the opposite is also common in many books, such as Kundur [12].

The flux linkage equations

$$\begin{bmatrix} \psi_d \\ \psi_D \\ \psi_{fd} \end{bmatrix} = \begin{bmatrix} L_d & L_{ad} & L_{fd} \\ L_{ad} & L_D & M_{fD} \\ L_{ad} & M_{fD} & L_{ffd} \end{bmatrix} \begin{bmatrix} -i_d \\ i_D \\ i_{fd} \end{bmatrix} \tag{3.3}$$

The set of equations above is expressing the relationship between flux linkages and currents in the d-axis, wherein ψ denotes flux linkage, L denotes inductance and i denotes current. Their subscript have the aforementioned association illustrated in Figure 3.2. Below are the equivalent-circuits of the inductances involved, showing their interconnection.

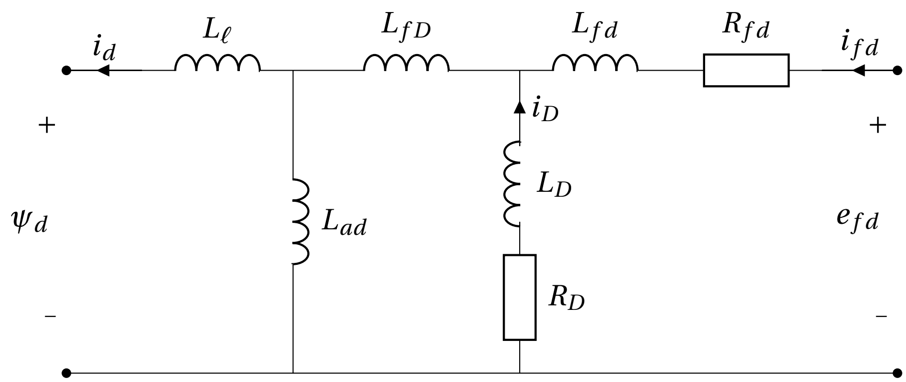

Figure 3.3: Per-unit d-axis equivalent circuit

The second set of the flux linkage equations in the q-axis:

$$\begin{bmatrix} \psi_q \\ \psi_Q \end{bmatrix} = \begin{bmatrix} L_q & L_{aq} \\ L_{aq} & L_Q \end{bmatrix} \begin{bmatrix} -i_q \\ i_Q \end{bmatrix} \tag{3.4}$$

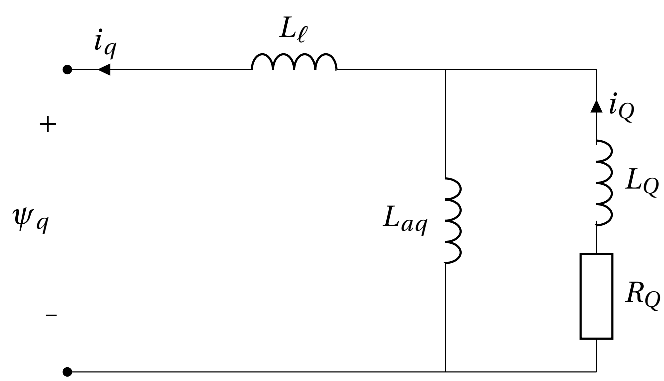

Figure 3.4: Per-unit q-axis equivalent circuit

The voltage equations

The following differential equations are describing the voltages in the synchronous machine:

$$u_d = -r_a i_d + \frac{d\Psi_d}{dt} - \omega\Psi_q \tag{3.5}$$

$$u_D = 0 = r_D i_D + \frac{d\Psi_D}{dt} \tag{3.6}$$

$$u_q = r_a i_q + \frac{d\Psi_q}{dt} + \omega\Psi_d \tag{3.7}$$

$$u_Q = 0 = r_Q i_q + \frac{d\Psi_Q}{dt} \tag{3.8}$$

$$e_{fd} = r_{fd} i_{fd} + \frac{d\Psi_{fd}}{dt} \tag{3.9}$$

wherein u denotes voltage and r denotes resistance. ω is the electrical speed speed.

The field voltage is given by the excitation system described later in this chapter. The damper winding voltages are always equal to zero, because they are short circuited and have no terminals (see Figure 3.2). Some models neglect the $\frac{d\Psi_d}{dt}$ and the $\frac{d\Psi_q}{dt}$ because their contributions are small. The armature resistance, r_a, may also be neglected dependent in some cases. None of these are neglected in the final model.

Electromagnetic torque equation

As the other equations, the electromagnetic torque is given in per unit:

$$T_e = (\Psi_d i_q - \Psi_q i_d) \tag{3.10}$$

The swing equation

All the aforementioned equations describes the electrical behaviour, while the following equation, also known as the swing equation, describes the mechanical motion:

$$T_{mech} - T_{em} = D\omega_m + 2H\frac{d\omega_m}{dt} \tag{3.11}$$

D denotes the damping constant (dependent on the damper windings), H is the per unit inertia constant. ω_m denotes mechanical speed of the rotor which is

$$\omega_m = \frac{d\theta_m}{dt} \tag{3.12}$$

resulting in

$$T_{mech} - T_{em} = D\frac{d\theta_m}{dt} + 2H\frac{d^2\theta_m}{dt^2} \tag{3.13}$$

The swing equation is explained further in appendix A.

Magnetomotive force (mmf)

The magnetomotive force (mmf) will be used in the derivation of the single-phase model. The fundamental armature mmf wave for the three-phase machine will therefore be presented:

$$\mathscr{F}_a = \frac{4}{\pi}\frac{k_w N_{ph(3)}}{2p}\frac{3}{2}\left[i_d cos(\delta) + i_q cos(\delta - \frac{\pi}{2})\right] \tag{3.14}$$

$\mathscr{F}_a$ is the mmf set up by the currents in the armature, where $k_w N$ is the number of turns per winding (k_w is the winding correction factor due to the winding distribution), p is the number of poles in the armature and δ is the rotor displacement angle .

3.4 The single-phase model

The method of modelling the single-phase model to be presented here is inspired by [19]. This method is employing the preexisting three-phase model equations in the dq-axis.

The single-phase model is obtained by first assuming the single-phase machine to be a two phase machine, using two of the stator windings. This is accomplished by simply loading the three-phase machine unsymmetrical, with load on two of the three phases, leaving the last phase unloaded. A single-phase system is achieved by connecting one of the two active phases to ground.

Hereby, this model will be called "the equivalent three-phase model".

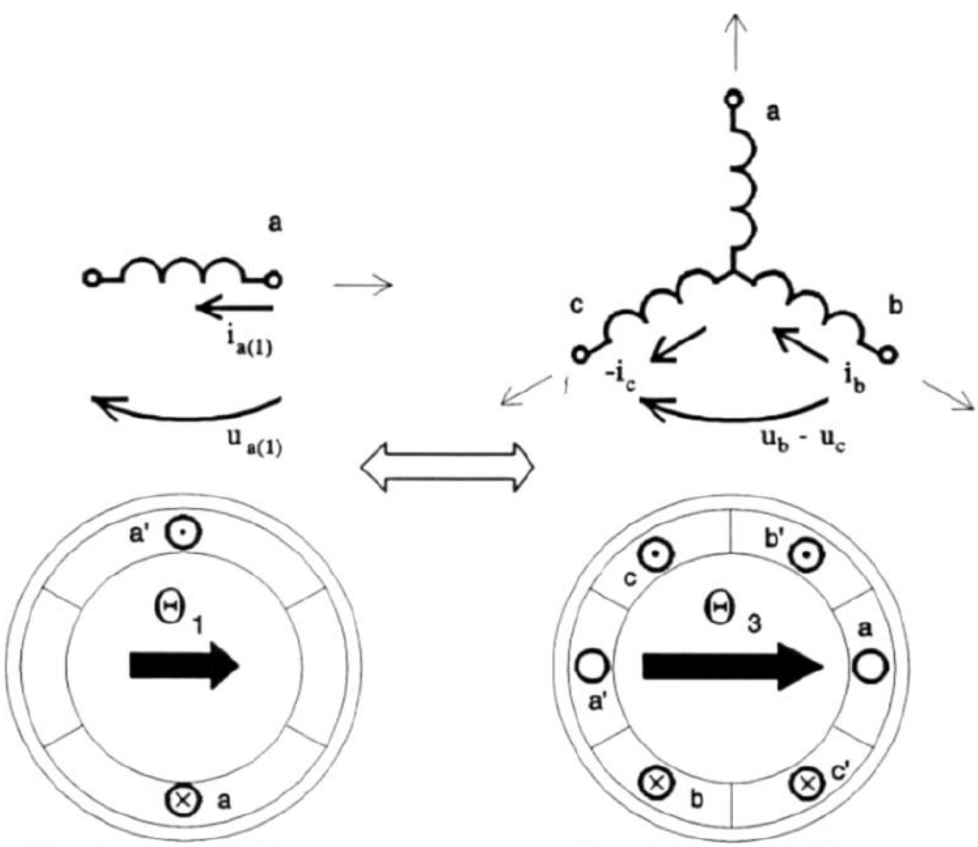

Figure 3.5: The single-phase winding on the left side and the equivalent three-phase windings on the right side. Θ is indicating the mmf. Figure taken from [19]

Since one of the armature windings is unloaded, the three phase currents are assigned as follows:

$$i_a = 0$$

$$i_b = i_1$$

$$i_c = -i_1$$

The single-phase voltage will then be:

$$u_1 = u_b - u_c$$

The subscript "1" is indicating the single-phase winding quantities as illustrated in the left part of Figure 3.5.

The armature flux from the single-phase winding will follow the same direction and be simultaneous in time to the three phase winding flux. The magnitude of the flux is dependent on the number of windings N and the current i. The electrical and magnetic conditions are the same in the three-phase and the single-phase, and also the interactions between these are the same. One of the main differences, is that the mmf is now not longer rotating, but pulsating. The magnetic field will remain stationary and generate pulses at twice the line frequency.

3.4.1 The single-phase currents in the dq-axis

The currents of the eq. three-phase model are $i_a = 0, i_b = i_1, i_c = -i_1$. The direct and quadrature axis currents are achieved by using the dq-transformation with the currents inserted:

$$i_d = \frac{2}{3} i_1 \left[0 + cos(\omega t - \frac{2\pi}{3}) - cos(\omega t - \frac{4\pi}{3}) \right] \tag{3.15}$$

$$i_q = -\frac{2}{3} i_1 \left[0 + sin(\omega t - \frac{2\pi}{3}) - sin(\omega t - \frac{4\pi}{3}) \right] \tag{3.16}$$

The β-coefficient mentioned in section 3.1 is selected to be $\frac{2}{3}$. With this coefficient, both the d- and q-axis armature windings have the same number of turns as an individual phase winding.

It is possible to do a simplification of the expression above using the following trigonometrical identities:

$$cos(\omega t-\frac{2\pi}{3})-cos(\omega t-\frac{4\pi}{3})= \\ \left[cos(\omega t)cos(\frac{2\pi}{3})+sin(\omega t)sin(\frac{2\pi}{3})\right]-\left[cos(\omega t)cos(\frac{4\pi}{3})+sin(\omega t)sin(\frac{4\pi}{3})\right] \quad (3.17)$$

Similarly with the Equation 3.16.

Because of the relations $cos(\frac{2\pi}{3}) = cos(\frac{4\pi}{3})$, $sin(\frac{2\pi}{3}) = \frac{\sqrt{3}}{2}$, and $sin(\frac{4\pi}{3}) = -\frac{\sqrt{3}}{2}$, the rearranged equation becomes:

$$i_d = \frac{2}{\sqrt{3}} i_1 sin(\omega t) \quad (3.18)$$

$$i_q = \frac{2}{\sqrt{3}} i_1 cos(\omega t) \quad (3.19)$$

MMF-equations in the single-phase machine

A descriptive way to see the physical relationships between a single-phase machine and its three-phase equivalent model is to have a look at the mmf (magnetomotive force) relationships.

According to Fitzgerald[1], the mmf wave of one phase winding can be resolved into a Fourier series, where the fundamental component is:

$$\mathscr{F}_{ph} = \frac{4}{\pi}\frac{k_w N_{ph}}{2p} i_{ph} cos(\theta-\theta_{ph}) \quad (3.20)$$

N_{ph} is the number of turns and k_w is the winding factor that takes into account the distribution of the winding. In the derivation of the equivalent three-phase machine equations, the notation $N_{ph(3)}$ will be used, and for the single-phase equations the notation $N_{ph(1)}$. As one can perceive, the mmf is varying with $cos(\theta)$ across the periphery of the stator, where θ indicates the space angle. The θ is defined as 0 degrees where the magnetic axis of the stator coil in phase a as in the Figure 3.6. From now, this is the reference zero.

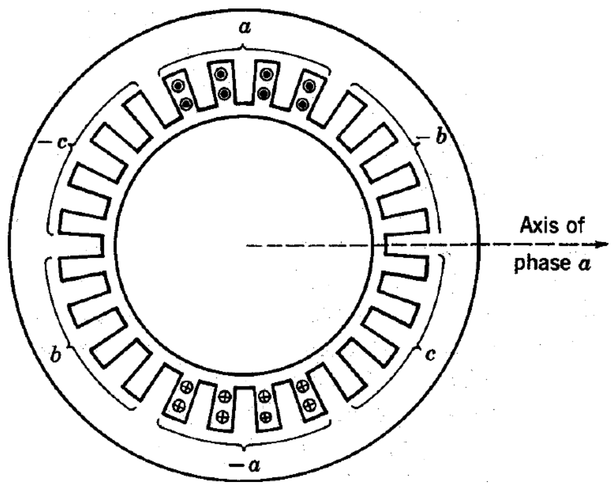

Figure 3.6: The magnetic axis of the stator coil in phase a in the equivalent three-phase system. Figure taken from [1]

The magnetic axis of the actual single-phase machine is defined to be 90 ° ahead of the magnetic axis of phase a in the equivalent three-phase machine above.

The space angle can be redefined to be an angle relative to the rotor angle

$$\theta = \omega_m t + \delta \tag{3.21}$$

Where $\omega_m t$ is the angle of the rotor, and the δ is the displacement relative to the rotor.

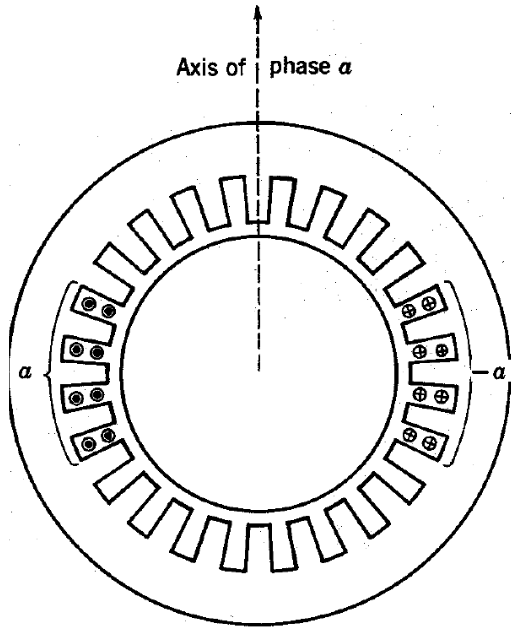

Figure 3.7: The magnetic axis of the single-phase winding (edited verson of Figure 3.6)

The mmf equation for the single-phase winding:

$$\mathscr{F}_1 = \frac{4}{\pi}\frac{N_{ph(1)}}{2p} i_1 cos(\omega t + \delta - \frac{\pi}{2}) \tag{3.22}$$

The magnetic axis is 90° ahead of the reference zero point, which is taken into account in the equation. The mmf will reach a maximum when $\theta = 90°$.

This equation can be divided into d and q axis components by setting the $\delta = 0$ in the d-axis, and $\delta = \pi/2$ in the q axis.

$$\mathscr{F}_{ad} = \frac{4}{\pi}\frac{N_{ph(1)}}{2p} i_1 cos(\omega t - \frac{\pi}{2}) \tag{3.23}$$

$$\mathscr{F}_{aq} = -\frac{4}{\pi}\frac{N_{ph(1)}}{2p} i_1 sin(\omega t - \frac{\pi}{2}) \tag{3.24}$$

Comparison of mmf-equations

The mmf-equation for the three-phase equivalent model is the same as in the standard model, which is stated in Equation 3.14. Inserting the transformed dq-currents from Equation 3.18 and

Equation 3.19 results in the following expressions:

$$\mathscr{F}_{ad} = \frac{4}{\pi}\frac{k_w N_{ph(3)}}{2p}\frac{3}{2}(\frac{2}{\sqrt{3}}i_1 sin(\omega t)) = \frac{4}{\pi}\frac{k_w N_{ph(3)}}{2p}\sqrt{3}i_1 cos(\omega t - \frac{\pi}{2}) \tag{3.25}$$

$$\mathscr{F}_{aq} = \frac{4}{\pi}\frac{k_w N_{ph(3)}}{2p}\frac{3}{2}(\frac{2}{\sqrt{3}}i_1 cos(\omega t)) = -\frac{4}{\pi}\frac{k_w N_{ph(3)}}{2p}\sqrt{3}i_1 sin(\omega t - \frac{\pi}{2}) \tag{3.26}$$

In order to make the "equivalent three-phase model" valid, Equation 3.25 and Equation 3.26 have to be equal to Equation 3.23 and Equation 3.24 respectively. By comparing the two equations, it can be seen that they are equal if the relation between the number of windings $N_{ph(1)}$ and $N_{ph(3)}$ is

$$N_{ph(1)} = \sqrt{3}N_{ph(3)} \tag{3.27}$$

This is an important result that will be used later in this report in the discussion of parameters.

The voltage equations

A single-phase machine has the following stator voltage equation:

$$u_1 = R_{(1)}i_1 + L_{\ell(1)}\frac{di_1}{dt} + \frac{d}{dt}\psi_1 \tag{3.28}$$

where

$$\psi_1 = N_{ph(1)}\Phi_1 = N_{ph(1)}\hat{\Phi}cos\big(\theta(t) - \frac{\pi}{2}\big) \tag{3.29}$$

Φ is indicating the flux. The same reference system is used, where the zero is the a-axis of the "equivalent three-phase model".

The stator voltage equations of phase b and phase c in the three-phase machine is:

$$u_b = R_{a(3)}i_b + L_{\ell(3)}\frac{di_b}{dt} + \frac{d}{dt}\psi_b \tag{3.30}$$

$$u_c = R_{a(3)} i_c + L_{\ell(3)} \frac{di_c}{dt} + \frac{d}{dt}\psi_c \tag{3.31}$$

With $i_1 = i_b = -i_c$, and $u_1 = u_b - u_c$ in the the three-phase equivalent model, the voltage can be expressed as:

$$u_1 = 2R_{a(3)} i_1 + 2L_{\ell(3)} \frac{di_1}{dt} + \frac{d}{dt}(\psi_b - \psi_c) \tag{3.32}$$

The flux linkages are defined as:

$$\psi_a = N_{ph(3)}\hat{\Phi_a} cos(\theta(t)), \quad \psi_b = N_{ph(3)}\hat{\Phi_a} cos(\theta(t) - \frac{2\pi}{3}), \quad \psi_c = N_{ph(3)}\hat{\Phi_a} cos(\theta(t) + \frac{2\pi}{3}) \tag{3.33}$$

By applying trigonometric identities and rearranging, the following is obtained:

$$\psi_b - \psi_c = \sqrt{3} N_{ph(3)}\hat{\Phi_a} cos(\theta(t) - \frac{\pi}{2}) \tag{3.34}$$

And the resulting voltage equation becomes:

$$u_b - u_c = 2R_{a(3)} i_1 + 2L_{\ell(3)} \frac{di_1}{dt} + \sqrt{3} N_{ph(3)} \frac{d}{dt}\Big(\hat{\Phi_a} cos(\theta(t) - \frac{\pi}{2})\Big) \tag{3.35}$$

Here, the 90 °alignment (mentioned earlier) is taken into account. The following can be written:

$$u_b - u_c = 2R_{a(3)} i_1 + 2L_{\ell(3)} \frac{di_1}{dt} + \sqrt{3} \frac{d}{dt}\Big(\psi_a\big(\theta(t) - \frac{\pi}{2}\big)\Big) \tag{3.36}$$

This result confirms the fact that the resistance over the single-phase armature winding equals the double of the three-phase winding.

$$R_{a(1)} = 2R_{a(3)} \tag{3.37}$$

The leakage inductance in the single-phase armature winding is the double of one winding in the equivalent three-phase model:

$$L_{\ell(1)} = 2L_{\ell(3)} \tag{3.38}$$

And the relation between the flux linkage of the single-phase winding and the flux linkage of one winding in the equivalent model:

$$\psi_1 = \sqrt{3}\psi_{a(3)} \tag{3.39}$$

which has the same meaning as in Equation 3.27.

The physical relations between the equivalent three-phase model and the single-winding model is now shown. The equations of motion will remain the same as in the three-phase model (Equation 3.13). Modelling a single-phase synchronous machine with the equivalent three-phase model requires that the relations shown above are satisfied. This may imply an adjustment in the parameters, which will be discussed in the next chapter.

3.5 Exciter and Automatic Voltage Regulator (AVR)

This section will deal with the models of the excitation system and the AVR.

Jernbaneverket is currently in the process of replacing the excitation systems on the rotating converters. The old DC excitation systems are being replaced with new AC excitation systems. The main reason for this is to improve the stability of the machines. Since all the measurements available are based on machines with the DC excitation system, the model in this thesis is based on the same system in order to make a correct comparative analysis.

The purpose of the excitation system is to provide direct current to the field winding (located in the rotor). Since the terminal voltage is strongly dependent on the field current, it is essential that the exciter and its accompanying regulator is ensuring voltage stability. IEEE has made some recommended models for modelling excitation systems[17], which will be used for the model in this thesis.

Model of the DC excitation system

The DC exciters for the machines in the rotary converters are identical, and of the type YGUA5. This regulator has been described thoroughly in the report *"2011021-11-2.0 Kompatibilitetsstudie för borstlös magnetisering"* [9], and the model presented here is based upon the information in this report.

Some changes and simplifications have been made compared to the model described in the aforementioned report (referring to the block diagram in "Bilaga 2"):

- The circuit related to K_D is removed since this is set to zero in the report
- The coupling related to the stabilizing feedback containing the parameters, K_F, T_F and T_M, has been slightly modified (due to stability problems in the attempt to implement this controller). This junction has been removed and replaced by a different feedback junction similar to the one used in the IEEE DC1A model [17].

The inputs of the model are (in p.u.):

- V_t - This is the terminal voltage, but it may otherwise be the output from the load compensator which is not included in this model.
- PSS - Signal from the power system stabilizer (PSS) signal. PSS is not included in the model.
- V_{REF} - Set point reference
- I_{fd} - Field current
- ω - Speed

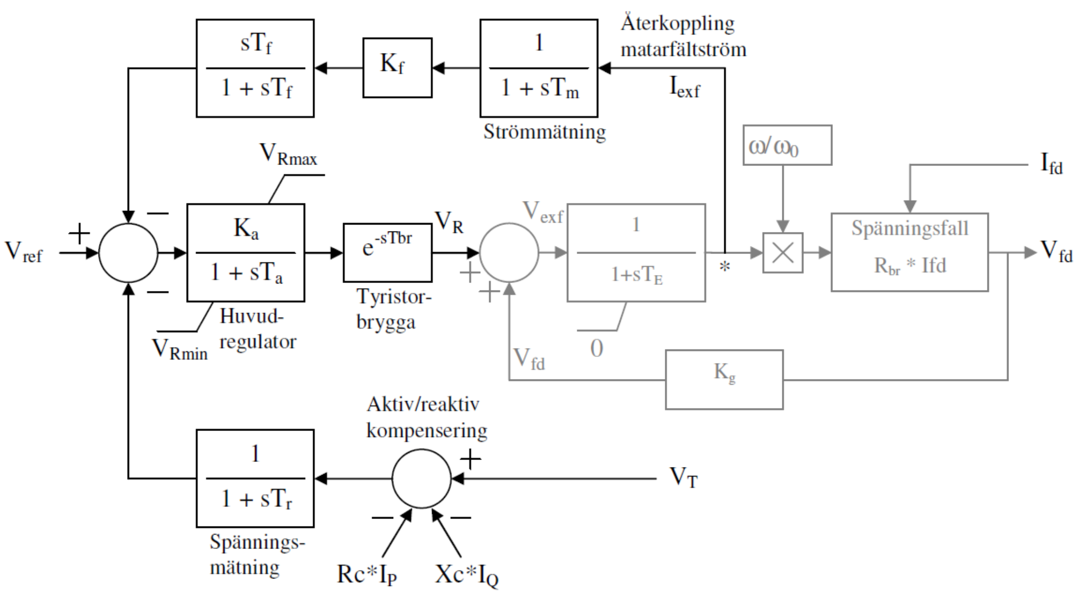

Figure 3.8: A simplified block diagram of the YGUA 5 DC excitation system, from the report "2011021-11-2.0 Kompatibilitetsstudie för borstlös magnetisering" [9]

The simplified block diagram depicted above is showing the DC exciter part in grey, while the regulator part is indicated in black. The the main regulator is of a standard type, and is followed by a time delay before it is entering the exciter part. The time delay is modelling the effect of having a thyristor bridge. The upper feedback loop has been modified slightly as mentioned above. The terminal voltage input, V_T, has a measurement time constant, T_r, representing the filtering and rectification of this signal. If needed, a load compensation component is added to the signal, but this is not included in the implemented model.

The diagram of the implementation in Simulink is depicted below.

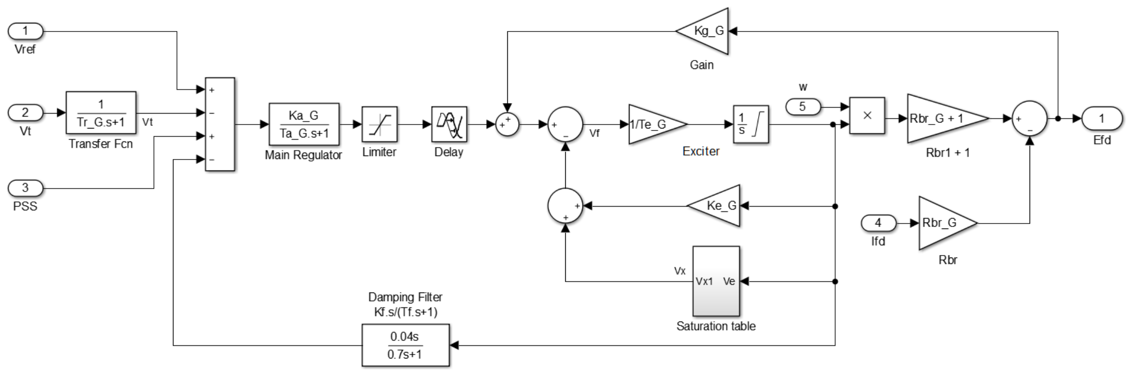

Figure 3.9: Block diagram of the YGUA 5 DC excitation system implemented in Simulink with some minor modifications"

Chapter 4

The parameters of the single-phase machine

This chapter will focus on the parametrization of the single phase machine. The previous chapter introduced the "equivalent three-phase model", which basically modelled the single-phase machine using a standard three-phase machine, with unbalanced loading at two of its three terminals. Using this method of modelling implies some adjustments of the original parameters.

4.1 The original parameters of the single-phase synchronous machine

The machine in question, which is the single-phase machine part of the rotary converter Q38, has the parameters stated in appendix B. Measurement data concerning the resistance of the stator is also available in appendix B.

These parameters are referred to as the standard parameters of a synchronous machine.

It is not known how these parameters were determined.

The following sections will present two alternative adjustment approaches.

The first will assume a calculation of machine parameters from design data, where the single-winding is the subject (as discussed in the last section).

The second will assume that the parameters are based upon a short-circuit test, where the determination has the same approach as in a standard three-phase synchronous machine.

4.2 Suggested adjustment based upon mathematical deduction

In order to employ the "equivalent three-phase model", the original parameters has to be adjusted to some extent. The adjustments of the synchronous inductances are not stated clearly in the Stoltze publication. A suggestion for these adjustments is presented here.

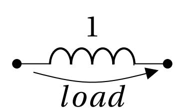

Figure 4.1: Original single-phase configuration

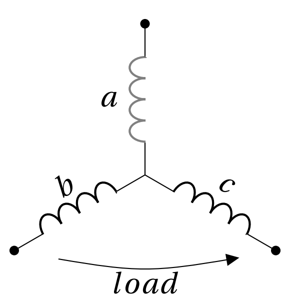

Figure 4.2: Three-phase equivalent configuration, with phase a left idle

Stator resistance - R_a

It was shown in chapter 3, and also by looking at the figures above, that the resistance in the single-phase winding is twice as large as the resistance in one three-phase winding :

$$R_{a(3)} = \frac{1}{2} R_{a(1)} \tag{4.1}$$

Leakage inductance - L_ℓ

The leakage inductance has the same relation as the stator resistance:

$$L_{\ell(3)} = \frac{1}{2} L_{\ell(1)} \tag{4.2}$$

Synchronous inductances - L_d **and** L_q

In equations 3.23,3.24,3.25,3.26,3.27, the following relation was derived:

$$N_{ph(1)} = \sqrt{3} N_{ph(3)} \tag{4.3}$$

In general, the number of turns in the armature is proportional to the mmf and the flux linkage produced by the armature.

These values are directly related to the *armature reaction inductance* and also the mutual inductance between the field and the armature winding (ref [7] p. 112). The use of $\beta = \frac{2}{3}$ in the derivation, makes this rate of turns one-to-one between the a-winding and the d or q winding.

The flux linkage equations is given in Chapter 3, and the following parameters have to be changed:

$$L_{ad(3)}, L_{fd(3)} \propto N_{ph(3)} = \frac{1}{\sqrt{3}} N_{ph(1)} \tag{4.4}$$

$$L_{aq(3)} \propto N_{ph(3)} = \frac{1}{\sqrt{3}} N_{ph(1)} \tag{4.5}$$

Assuming the original parameters are determined on a single winding basis, the following relations becomes valid:

$$L_{ad(3)} = \frac{1}{\sqrt{3}} L_{ad(1)} \tag{4.6}$$

$$L_{fd(3)} = \frac{1}{\sqrt{3}} L_{fd(1)} \tag{4.7}$$

$$L_{aq(3)} = \frac{1}{\sqrt{3}} L_{aq(1)} \tag{4.8}$$

The definition (from [12]) of the synchronous inductance is:

$$L_d = L_{ad} + L_\ell \qquad L_q = L_{aq} + L_\ell \tag{4.9}$$

From what is stated above, the resulting synchronous reactance becomes

$$L_{d(3)} = \frac{1}{\sqrt{3}} L_{ad(1)} + \frac{1}{2} L_{\ell(1)} \qquad L_{q(3)} = \frac{1}{\sqrt{3}} L_{aq(1)} + \frac{1}{2} L_{\ell(1)} \tag{4.10}$$

Transient inductance - L'_d

The transient inductance is dependent on the field winding, and since there is no field winding in the q-axis, the L'_q is normally not included as a parameter. The definition of the transient inductance (from [12]) is

$$L'_d = L_\ell + \frac{L_{ad} L_{fd}}{L_{ad} + L_{fd}} \tag{4.11}$$

From the relations stated above, the new transient inductance can be expressed as:

$$L'_{d(3)} = \frac{1}{2} L_{\ell(1)} + \frac{1}{\sqrt{3}} \Big(\frac{L_{ad} L_{fd}}{L_{ad} + L_{fd}} \Big)_{(1)} \tag{4.12}$$

Subtransient inductances - L''_d and L''_q

According to Kundur, the subtransient inductance is the following:

$$L''_d = L_\ell + \frac{L_{ad} L_{fd} L_{1d}}{L_{ad} L_{fd} + L_{ad} L_D + L_{fd} L_D} \tag{4.13}$$

The damper winding inductance, L_D, remains unchanged in the three-phase equivalent model. The resulting transformation becomes:

$$L''_{d(3)} = \frac{1}{2} L_{\ell(1)} + \frac{1}{\sqrt{3}} \frac{L_{ad(1)} L_{fd(1)} L_{1d}}{\big(\frac{1}{\sqrt{3}} L_{ad(1)} L_{fd(1)}\big) + L_{ad(1)} L_{1d} + L_{fd(1)} L_{1d}} \tag{4.14}$$

The subtransient inductance in the q-axis can be expressed as:

$$L''_q = L_\ell + \frac{L_{aq} L_Q}{L_{aq} + L_Q} \tag{4.15}$$

Which becomes:

$$L''_{q(3)} = \frac{1}{2} L_{\ell(1)} + \frac{\frac{1}{\sqrt{3}} L_{aq(1)} L_Q}{\frac{1}{\sqrt{3}} L_{aq(1)} + L_Q} \tag{4.16}$$

The standard synchronous machine parameters are given in per unit value in steady state. With $\omega_0 = 1$, the reactance becomes identical to the inductance.

4.3 Open-circuit time constants - T'_{d0}, T''_{d0} and T''_{q0}

The time constants can either be measured in open-circuit or short circuit. Because the open circuit time constants are the ones stated in the parameter list, they are the ones that will be considered here.

The d-axis transient open-circuit time constant is only dependent on parameters of the field winding:

$$T'_{d0} = \frac{L_f}{R_f} \tag{4.17}$$

L_f and R_f are the inductance and the resistance of the field winding. The changes in the equivalent three-phase machine are only related to the armature winding, so the d-axis transient open-circuit time constant will remain at the same value.

The time constant for the subtransient state is representing the decay of current in the damping winding, and is defined (in [7]):

$$T''_{d0} = L_D - \frac{L_{fD}^2}{L_f} \frac{1}{R_D} \tag{4.18}$$

And for the q-axis:

$$T''_{q0} = \frac{L_Q}{R_Q} \tag{4.19}$$

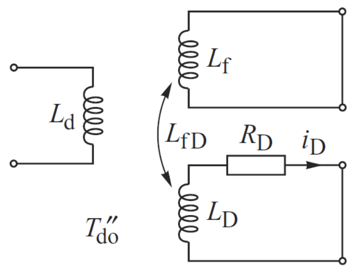

Figure 4.3: Equivalent circuit of the d-axis inductances

Again, the parameters involved are not related directly to the armature winding. The L_D and L_Q are representing the inductance of the damper windings while R_D and R_Q represents the resistance.

It is therefore no reason to change the time-constants from the original parameters.

4.4 Table of original and adjusted parameter values

The relations expressed in the last section makes it possible to calculate the new adjusted values for the equivalent three-phase machine. In the table below, the original parameters are taken from the Q38 rotating converter. This contains a single phase synchronous machine with a $4MVA$ rated apparent power and $4kV$ nominal voltage. The parameters are the ones found in Danielsen [4].

Table 4.1: Table of the original and adjusted parameters in per unit

Parameter	Original value	Adjusted value
X_d	1.02	0.582
X_q	0.47	0.264
X'_d	0.12	0.062
X''_d	0.10	0.050
X''_q	0.11	0.052
R_a	0.0044*	0.0022
L_ℓ	0.096	0.048
T'_{d0}	8.6	8.6
T''_{d0}	0.08	0.08
T''_{q0}	3.4	3.4

* The armature resistance in [4] is 0.0175 and this claimed to be in per unit. If one look at the reports of armature resistance measurements (in appendix B), they are stated to be in the area 0.017-0.018 ohm. It is assumed that the statement in [4] is meant to be in ohms, and this value transformed into the per unit basis becomes 0.0044.

4.5 Determination of parameter values from sudden short-circuit test

A well established method of determining the parameter values of a synchronous machine is by measuring its sudden short-circuit current. Performing this test on a three-phase machine implies a three-phase bolted short-circuit where all three phase terminals are connected to ground simultaneously. The resulting short-circuit current will give a foundation for determining the parameters.

Although the method for determining the parameters of single-phase synchronous machine in question is unknown, it will here be made an assumption.

It will be presumed that the parameters of the single-phase machine is based upon a sudden short-circuit test. The evaluation of the parameters are assumed to be done in the same way as of a standard three-phase synchronous machine.

The situation is now comparable with the "equivalent three-phase model". This case is actually a two-phase-to-ground fault, while the reference case is a standard three-phase-to-ground fault.

A comparison of these can be seen below:

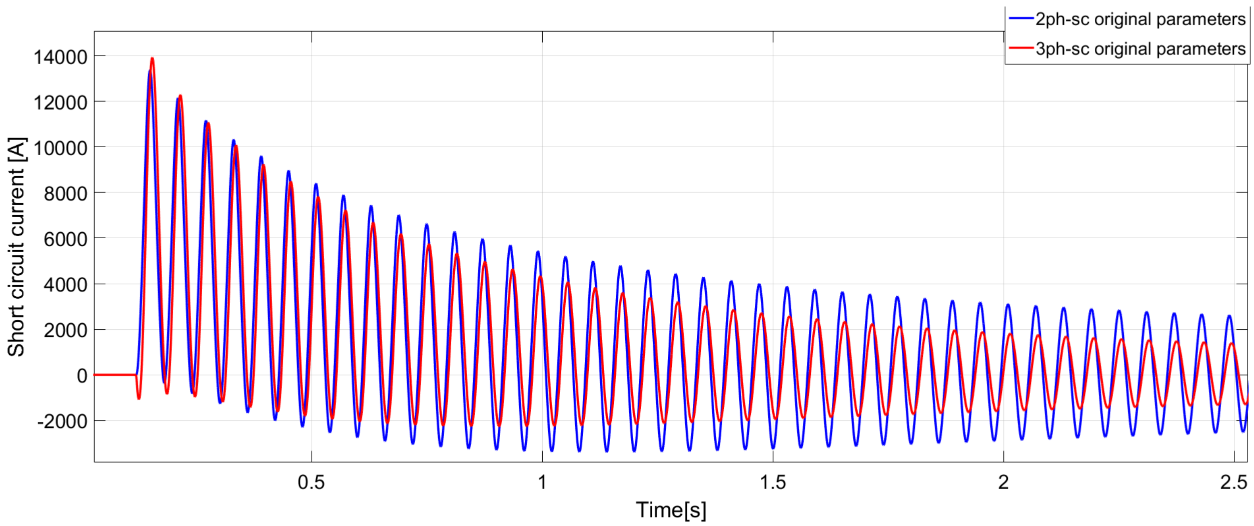

Figure 4.4: Simulated comparison between a 2ph-to-ground (in blue) and a 3ph-to-ground (in red) sudden short-circuit (at the zero-crossing of the voltage) on a standard three-phase synchronous machine model. Measured on phase b. The parameter values are identical in both cases. The short-circuit is located directly at the machine terminals.

As seen from the figure, and as expected, there is a deviation in both the sub-transient, transient and steady state current. The original parameters are applied in both of the two cases. With the assumptions made above, it is the 3ph-to-ground short circuit which is the the characteristic that describe the actual machine. In this case, it will be possible to adjust the parameters of the equivalent three-phase model in order to make it fit the 3ph-to-ground characteristic.

An experimental approach was chosen, and some adjustment was found to be successful: Multiplying the synchronous reactances with $\sqrt{3}$, increasing transient reactances with 5% and reducing subtransient reactances with 5% :

Table 4.2: Table of the original and adjusted parameters in per unit

Parameter	Original value	Adjusted value
X_d	1.02	$\sqrt{3}$*1.02
X_q	0.47	$\sqrt{3}$*0.47
X'_d	0.12	1.05*0.12
X''_d	0.10	0.95*0.10
X''_q	0.11	0.95*0.11

A new comparison is made, with the adjusted parameters in the 2ph-to-ground, keeping the orignal parameters in the 3ph-to-ground.

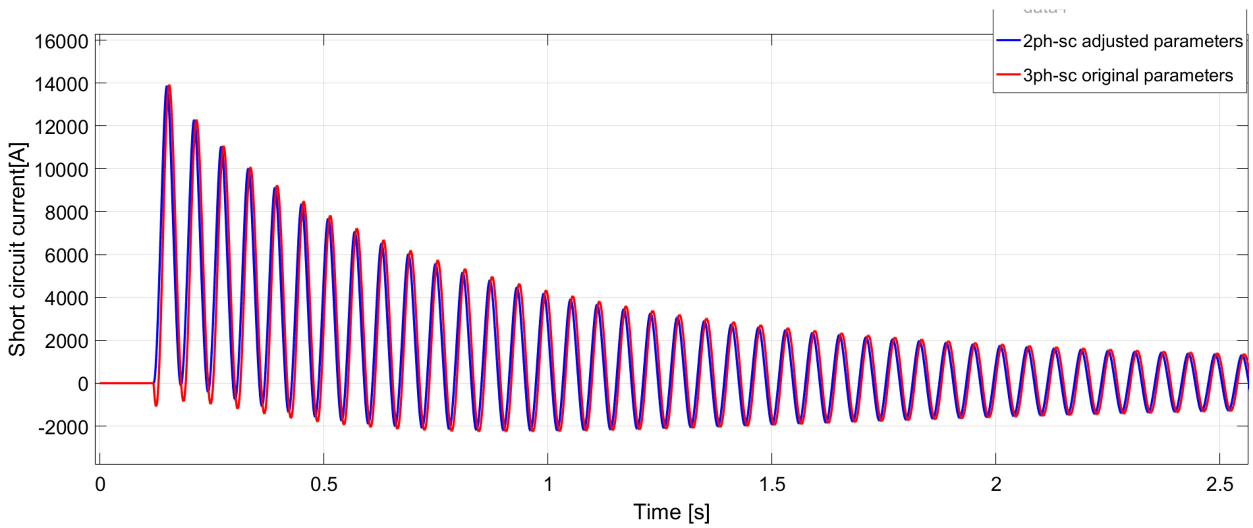

Figure 4.5: Simulated comparison between a 2ph-to-ground (blue) and a 3ph-to-ground (red) sudden short-circuit (at the zero-crossing of the voltage) on a standard three-phase synchronous machine model. Measured on phase b. The parameters adjusted in the 2ph-ground case, while 3ph-ground is with original parameters. The short-circuit is located directly at the machine terminals.

The two cases have now nearly the same characteristic.

Chapter 5

The implementation of the mathematical model in Simulink and Simpow

A model is a mathematical representation of a theory that can be used to calculate a prediction of an outcome in reality. The model will imitate the characteristic of the process in question, which in this case is an electrical machine. After the model is formulated, it is time to test the validity of the model through dynamic simulation which is accomplished by using a simulation software tool. This chapter will emphasize how the model has been realized in the chosen simulation software.

5.1 Simpow

Simpow is a powerful software tool developed by ABB. It may be employed for dynamic simulations of various electrical power systems.

In Simpow, there are two main modules which are *Optpow* and *Dynpow*. The *Optpow* module is for power flow simulations and steady state conditions, while *Dynpow* can simulate in time domain. *Dynpow* has an instantaneous value mode which is called *MASTA*, and also a RMS-value mode which is called *TRANSTA*. Today there excists a model of a single-phase machine in the *TRANSTA*-mode, but not in the *MASTA*. This missing *MASTA*-model, an instantaneous value model of a single-phase synchronous machine, was requested by Jernbaneverket.

Due to some difficulties and problems related to the software, the implementation discontinued and another software tool was considered.

Anyhow, Simpow has been used for some simulations in the comparative analysis done in the next chapter.

5.2 The Simulink/MATLAB model

Simulink is a simulation toolbox extension included in the MATLAB software package, and was chosen as the main simulation tool in this thesis due to its rich library and flexible functionality. In the library "Simscape Specialized Technology", one can find premade standard models of synchronous machines, AVR and other components.

5.2.1 Synchronous machine model

The single-phase machine has been modelled as a standard synchronous machine (IEEE model 2.1 in Figure 3.1), and this model can be found in the "Simscape Specialized Technology" library. The electrical part of the machine model is of sixth order, losses and saturation is neglected.

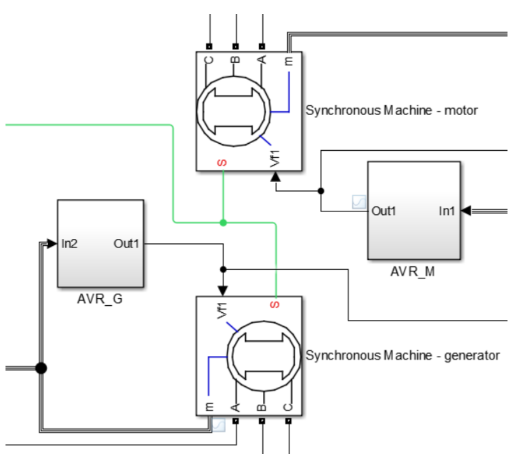

Figure 5.1: Synchronous machine blocks connected together as in a rotating frequency converter, from the Simulink model

The inputs of the block are

- *The three-phase terminal ports (A, B, C)*, where phase *a* is left idle in the single-phase machine. For numerical reasons, a large resistance ($1M\Omega$)is connected to each of the terminal inputs.
- *Mechanical rotational port (S)*, representing the rotor shaft. This port makes it possible to interconnect the machine model with other machine models, which is the case in a rotating frequency converter. This is utilized in the model where the two synchronous machine blocks are connected together.
- *Field voltage (Vf1)*, is usually connected to a AVR-block, or in some cases just a constant signal/value.

Simplifying assumptions made in the synchronous machine model

- Perfect symmetry of windings
- Sinusoidal distribution of magnetomotive force (mmf)
- Absence of magnetic saturation and hysteresis (magnetic linearity assumed)
- Inductances are constant
- No mechanical loss (friction)
- No heating effects

5.2.2 Automatic Voltage Regulator and Exciter

The "Specialized Technology" library in Simulink contains various sorts of standardized excitation systems, such as *DC1A*, *AC1A* , *ST1A* and more.

The *YGUA5* excitor was implemented, but run unsuccessfully, it did not stabilize the voltage and led to a unstable system. The *DC1A* was able to stabilize the voltage. It was therefore desired to employ this block instead, and it has been used during all the simulations.

5.2.3 Transformers

There are two transformers used in the model, the one on the motor side and the one on the generator side. Simulink has a standard block representing simple two-winding transformer.

The parameter for the transformer in [4] is only given as one single impedance. The Simulink block is requiring one impedance for winding 1, and one impedance for winding 2, given in per unit. Since these are in per unit, no consideration needs to be made with the turn ratio. The total equivalent impedance of the transformer (according to [3]) is the sum of the winding impedances. This has been solved by having half of the equivalent impedance (in per unit) on each of the windings.

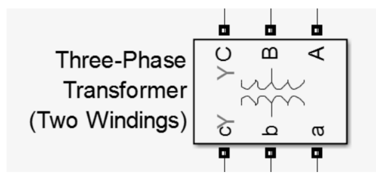

Figure 5.2: Single-phase block of the three-phase two winding transformer

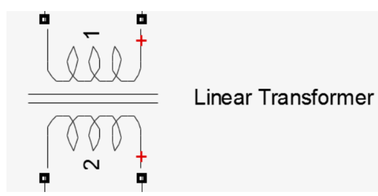

Figure 5.3: Single-phase block of the three-phase two winding transformer

5.2.4 Stiff grid

In the model (and in reality) the rotary converter is connected to the main grid. This grid is robust and stiff, and is considered as the slack bus (reference bus). In Simulink, this is accomplished by using an ordinary three-phase source and setting it to be the swing bus.

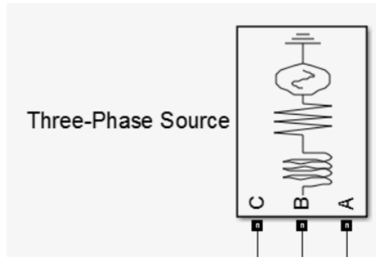

Figure 5.4: Ordinary block of a three-phase source

5.2.5 The complete model in Simulink

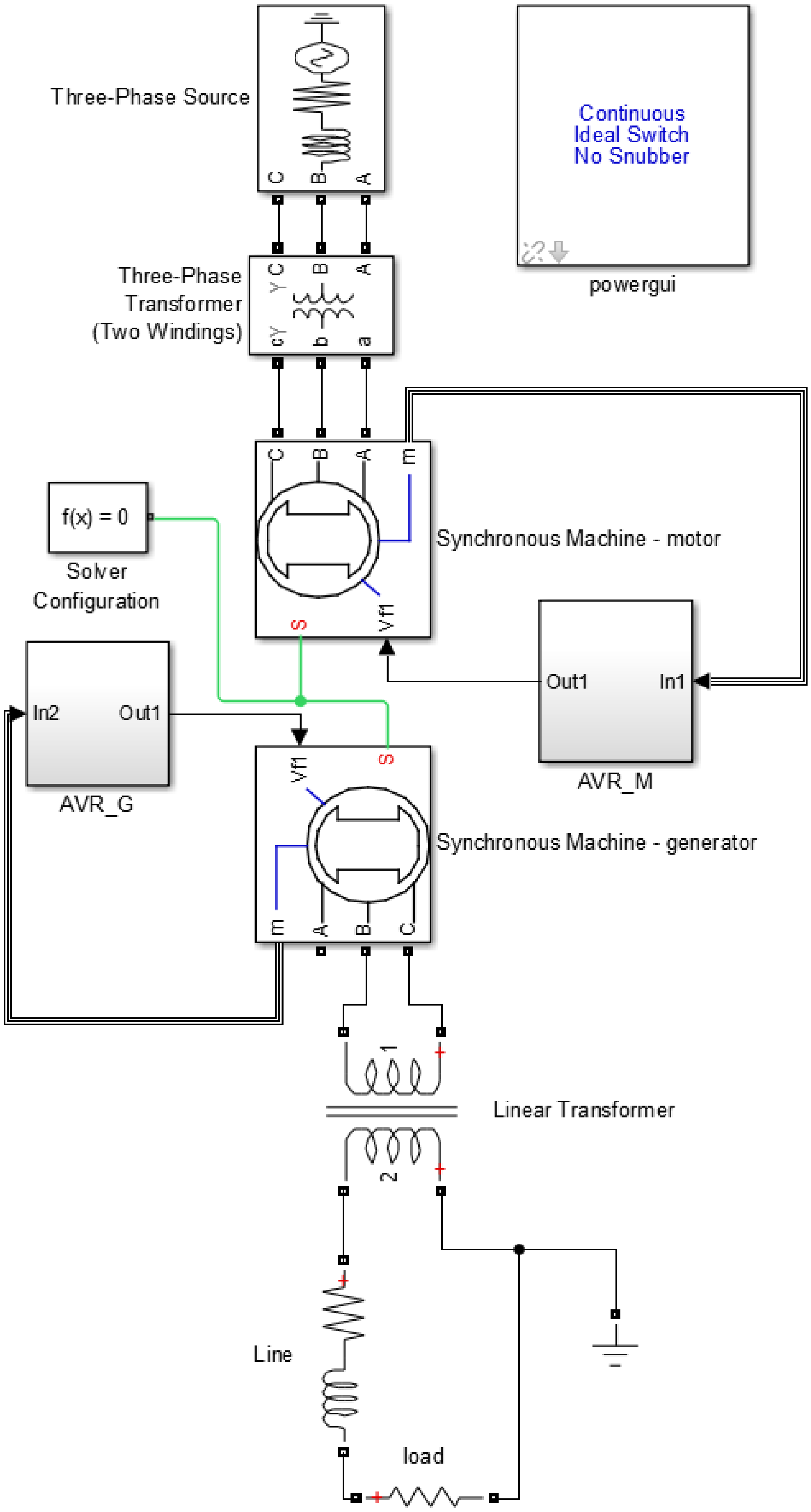

Figure 5.5: All the blocks connected in Simulink

5.2.6 Solver

Regarding the numerical solving method, a continuous solver with variable step has been chosen, compromising the computation time and allowing higher accuracy. The solver used is called "ode15s", and is a variable step, variable order solver.

A quicker calculation could be obtained by choosing a discrete solver. Attempts were made with such solver, but the results were found unsatisfying due to jagged scope data and low accuracy.

Chapter 6

Results of simulations and discussion

A good way to check the validity of the model is to compare the results with genuine measurements of the actual system. The simulations in this chapter will emphasize on a few cases where there is existing measurement data.

6.1 Cases

The simulation cases will be presented, the simulations and comparison for the respective cases with a consecutive discussion of the results. All the simulations is carried out in island mode, where the rotating converter is supplying the load alone. The three-phase synchronous motor is supplied from a 66kV stiff grid through a transformer. It is used a 230 Ω resistor as a load, in the cases run with load. All the parameter values for the cases can be found in appendix B.

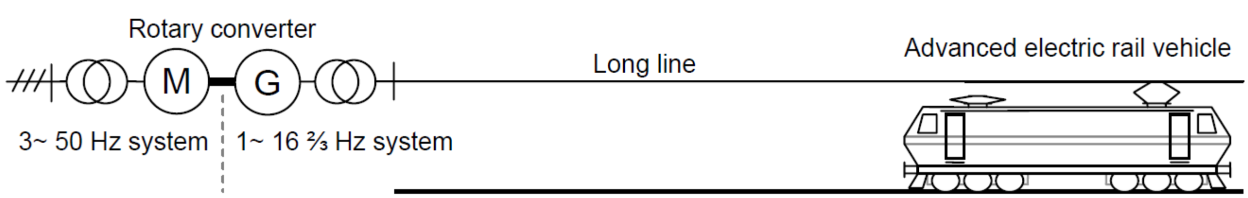

Figure 6.1: A simple sketch of the setup in all the simulations. "Advanced electric rail vehicle" is represented only with a resistive load. Figure taken from [4]

6.1.1 Case 1 - Load step-down response test

The first set of measurements recieved from Jernbaneverket is concerning a step-down in load, from ca. 1.2 MW to 0 MW. The test was performed at Hønefoss converter station, with the converter in island mode. It supplies a train, which accelerates until the main circuit breaker is opened. The measurements in this case is only containing RMS values.

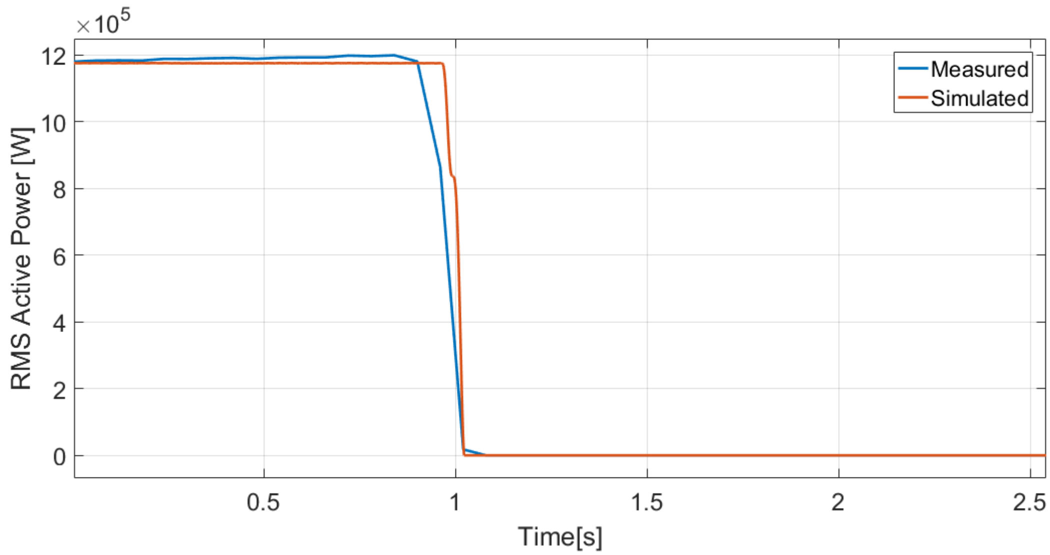

Figure 6.2: The plot is showing the step in active power

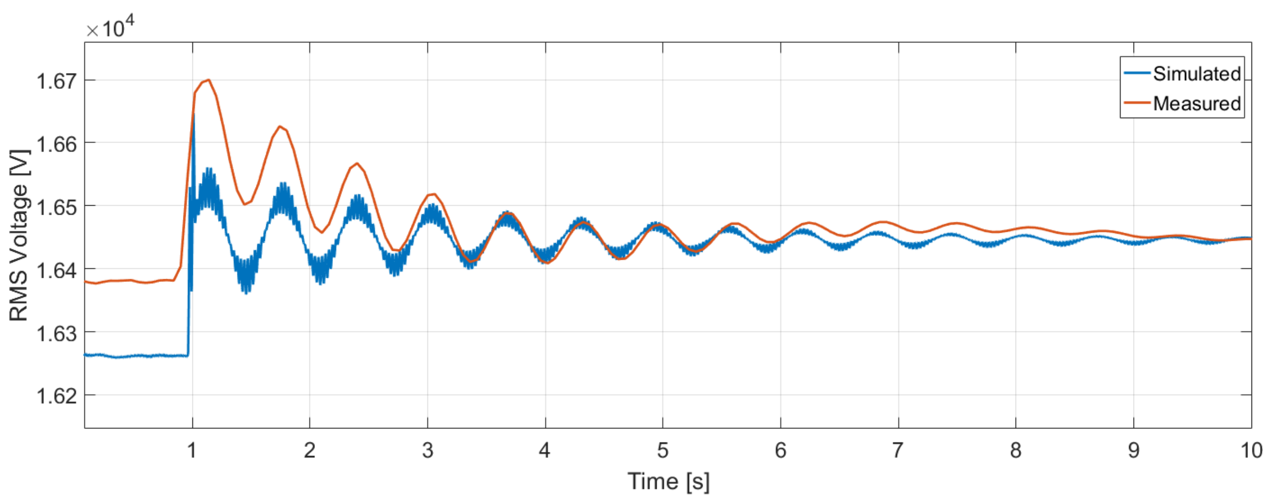

Figure 6.3: Step response in the RMS voltage

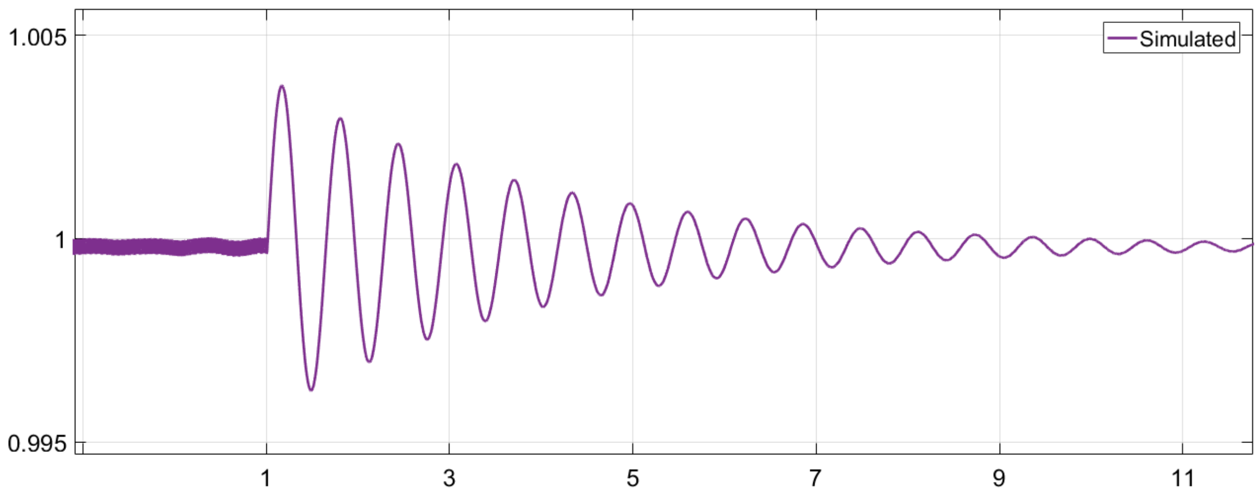

Figure 6.4: The rotor speed response in per unit (only simulation). The natural oscillation frequency is measured to 1.5 Hz.

The intention of this test is to show the natural oscillation frequency in the rotary converter. The natural oscillation following a change in load, is a well known phenomenon which is discussed in [20] and [4]. This can be seen in Figure 6.4. The oscillation frequency is 1.5 Hz, which is close to the measured frequencies in [4]. This oscillation has an effect on the voltage, which is observable in the RMS voltage in Figure 6.3.

In the plot of the RMS-voltage, one can see that the oscillation frequency is present in both the measured and the simulated response, and that they are interfere with each other. Although, there is some deviation, which may be because they are using different AVRs. In the model, the DC1A block is employed, while an YGUA5 type AVR is used on the actual machines.

Another observation worth mentioning, is the voltage during the preliminary period, when the load is still connected. The voltage in the simulation is about 100 Volts lower than in the measurement. This is perhaps because the model has a larger line impedance or transformer impedance than in reality, even though the same line length (5km) is used in calculating the line impedance.

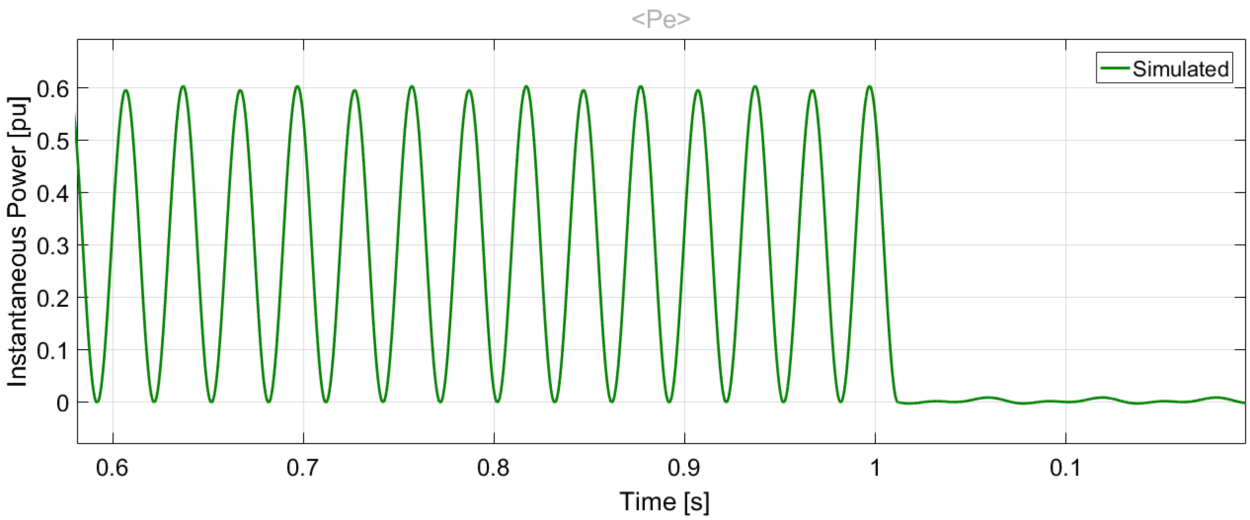

Figure 6.5: The instantaneous active power in per unit from the single-phase synchronous machine (only simulation), with frequency 33 Hz.

Figure 6.5 is included to illustrate that the instantaneous power is pulsating at twice the line frequency, as mentioned in chapter 2. Unlike the instantaneous power in a standard three-phase machine, where it is ideally continuous and not pulsating.

6.1.2 Case 2 - Short circuit current

A short circuit test has been performed by Jernbaneverket on a Q38 rotating converter, and the measurements of this is the basis for the comparative analysis in this section. The short circuit was located close to the converter, but after the transformer. The field voltage is kept at its nominal value during the short circuit.

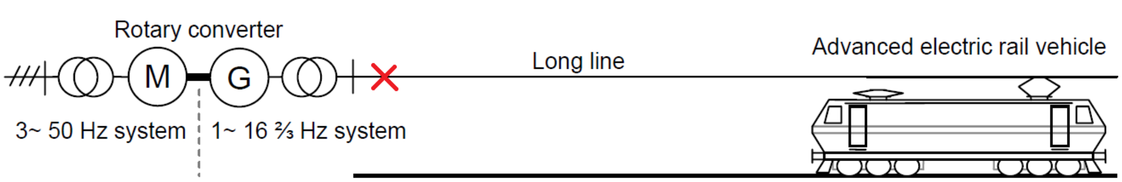

Figure 6.6: The red cross is indicating the location of the short circuit test. Figure taken from [4]

Unfortunately, the short circuit test was not initiated at the voltage zero point, but almost at the voltage max point. This has been taken into consideration, and the initiation point of the simulation has been carefully adjusted to make it as similar to the measurement as possible.

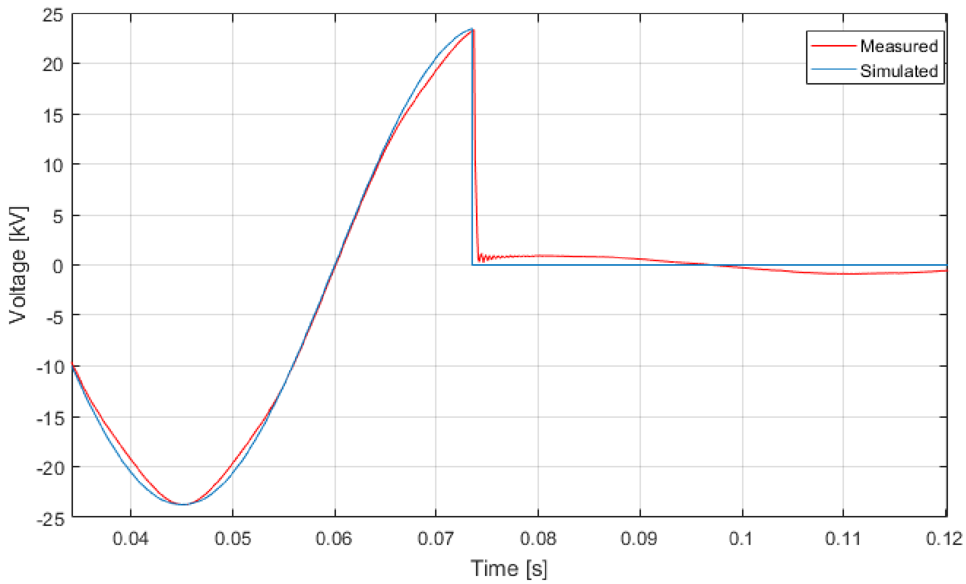

Figure 6.7: Plot of the voltage during the short circuit, showing simulation versus measurement

As the parameter values are of importance for the results, different sets of parameters were tested.

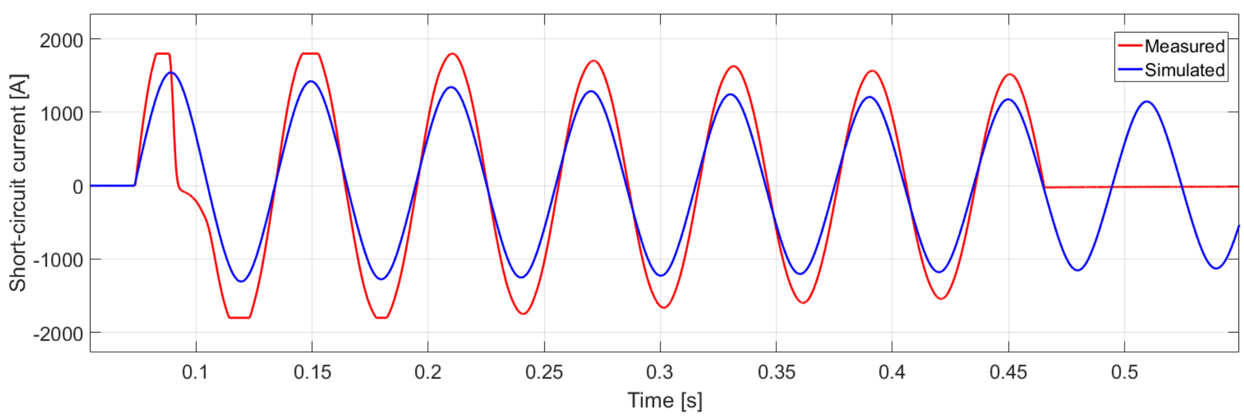

Figure 6.8: Plot of the short circuit current, using the original set of parameters with no adjustments made

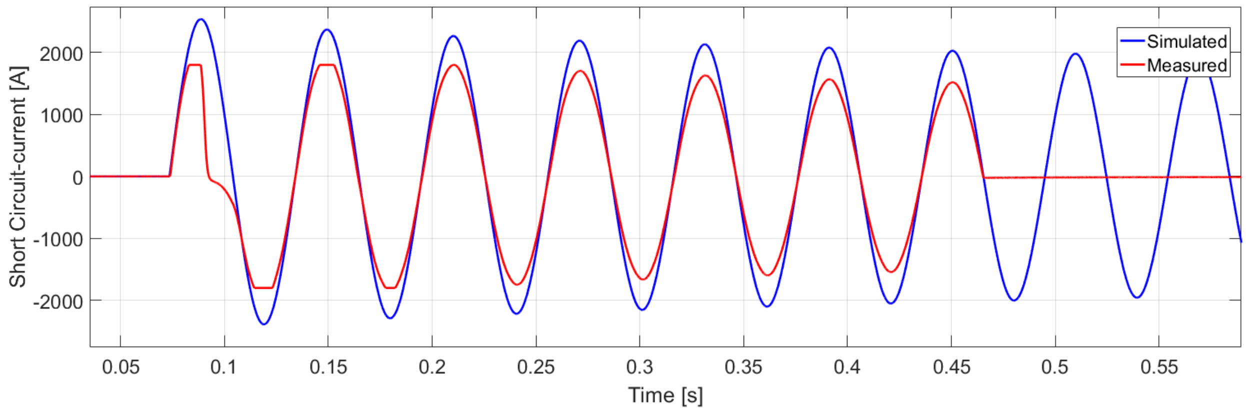

Figure 6.9: Plot of the short circuit current, adjusted according to the first set of adjusted parameter values in chapter 4 (Table 4.1)

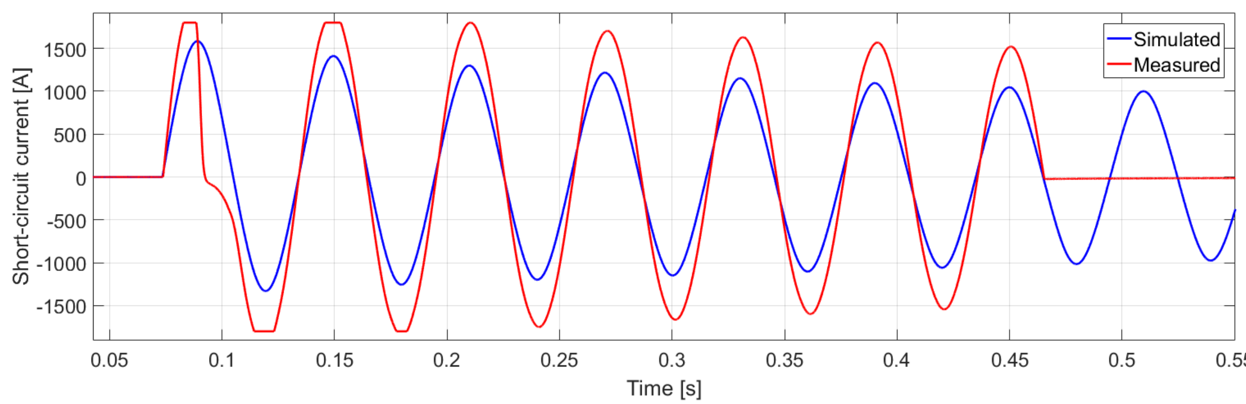

Figure 6.10: Plot of the short circuit current, parameter values adjusted according to Table 4.2

A new set of parameter values was also tested. These parameters were determined on experimental basis, with the aim of making the simulation fit the measurement. Only the synchronous reactances are changed, where the original values are reduced with 30%.

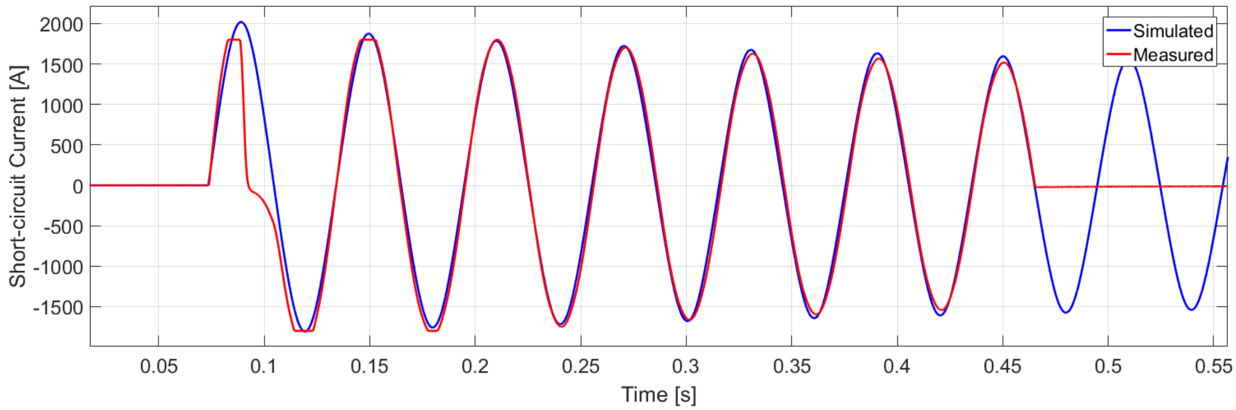

Figure 6.11: Plot of the short circuit current, where the parameter values was adjusted after some experimentation (with a factor of 0.7)

The measurements has some cut-off in the first periods, and are only lasting for about 0.4 seconds. This gives opportunity to verify the subtransient and the transient state, to some extent. Another important issue is that the short-circuit is located after the transformer, which means that the impedance of this has to be included. Its exact value is not known, the parameters for the transformer in the model is taken from [4]. The value of the transformer will have a great impact on the resulting short-circuit current. Because of this uncertainty, none conclusions can be made from a comparison of measurements and simulations. It is assumed that the transformer parameter is correctly set.

The original parameters are applied in the first comparison viewed in Figure 6.8. One can see that the short-circuit current has a lower amplitude than the measurements, where the simulation is about 25% lower in the first periods compared to the measurement. This difference is slightly reduced in the last period to 23%. In general, both curves seem to follow the same trend.

The second comparison is with the first set of adjusted parameters as stated in Table 4.1. Here the situation is opposite, the short-circuit current in the simulation has a larger amplitude than in the measurements. The amplitude is 26% higher in the third period, increasing to 33% in the last period. It is impossible to judge the first periods of the measurement, as they are cut-off.

In the third comparison, the experimental parameters from chapter 5 is considered. In this case the reactances are increased, which results in a lower current, and as expected the simulations shows a lower current than the measurement. In the third period, the difference is 28%, while in the last it is 32%.

In the final simulation, some other experimental parameters were taken into trial. All the reactances ($X_d, X_q, X_d', X_d'', X_q''$) where reduced with 30%. The difference between the two curves are now small, with only 1-2% in the beginning, and 5% in the last period.

Another key point in these short-circuit simulations is the firing angle, the timing point of the short circuit. This has great importance of the results. In the aftermath, it was found that the point of the short-circuit could be done 0.5 ms later according to the comparison of the voltage lapses.

6.1.3 Case 3 - Comparison with the Simpow model

In the third case, it will be made comparisons with the Simpow model. The Simpow model is only able to output RMS-values.

In this case it will be performed a simple no-load short circuit, similar to the one in Case 2, only here outputting the RMS short-circuit current. The short circuit is located directly at the generator terminals, unlike in Case 2, where it was located after the transformer.

It is to be mentioned that if one change the single-phase model in Simpow into a three-phase model (which is done easily in the optpow-file), one will obtain the exact same short circuit current characteristic. It seems as if the three-phase model and the single-phase model are the same model in Transta mode (RMS mode).

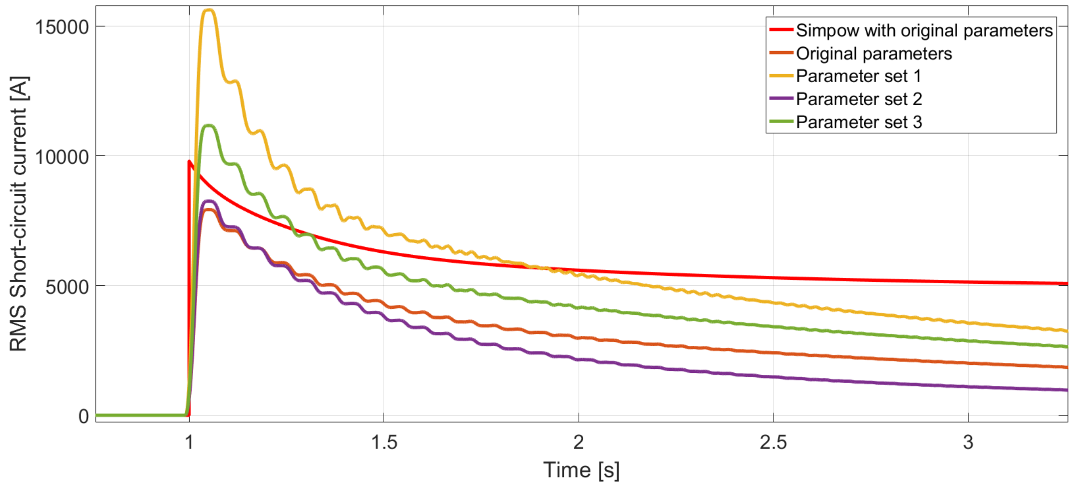

Figure 6.12: Plot of the RMS short circuit current, Simulink simulations compared with the simpow simulation. No initial load.

Parameter value set 1 is the first set of parameter values in chapter 4, while set 2 are the second, in addition to parameter set 3, which is the one found in this chapter (0.7 on all reactances).

It can be seen that there is a dismatch between the characteristics. None of the sets of parameter values are able to reflect the Simpow characteristic.

Chapter 7

Conclusions

A method of modelling single-phase synchronous machines has been developed and presented. The model is of fairly simple nature. It is easy to implement and incorporate with an preexisting standard three-phase model, by simply loading two of its phases and leaving one phase idle. This method is also recommended by [19] and [14].

This model was implemented in Simulink by using standard model blocks found in the software library.

It has been suggested that this method of modelling requires a change in the parameters. Three sets of new parameters have been presented. These have been applied to the model and short circuit simulations have been carried out. The results were compared with the measurements. But since the measurements are insufficient, it is impossible to confirm the validity of the parameters. It has neither be confirmed whether a change in parameters is necessary or not. Anyhow, it has been seen that with an adjustment of the parameter values, one can achieve results that are quite close to the measurements.

It has been proven a strong similarity between the simulations and the measurements. The dynamic behaviour and the overall operation of the model has shown to be reflecting the general behaviour of the rotary converter.

7.1 Further work

It is observed that there is still some work remaining. Here are suggestions for further work:

- More effort could be made in making the model identical to the single-phase machine. This can be achieved with the right adjustment of the parameters. In order to clarify the parameter adjustment, more thorough measurements are required. Effort could be made in doing an enhanced sudden short-circuit test directly on the terminals of the single phase synchronous machine.
- An other way to find the right parameter adjustment could be to dive into the mathematical model of the machine and search for another deduction.
- It was attempted to implement a model of the YGUA5 AVR. Although, the implemented model had stability issues. Effort could be made into making this model work faultlessly.
- The model calculation time of the simulation in Simulink is rather slow. Work could be put into finding a better solver that is able to calculate the values in less time, while the result remains adequate.
- The model was originally meant for being implemented in the Simpow simulation software. Now that a working model exists in Simulink, it should be possible to implement it in Simpow. It would be possible to extract the code of the Simulink-model and then adopting it to DSL-code.

Bibliography

[1] Stephen D. Umans A. E. Fitzgerald, Charles Kingsley Jr. *Electric Machinery - Fifth Edition*. Mc Graw Hill.

[2] T. A. Rogers B. L. Robertson. *Performance of the Single-Phase Synchronous Machine*. AIEE TRANSACTIONS, 1947.

[3] Stephen J. Chapman. *Electric Machinery Fundamentals - Fourth Edition*. McGraw Hill, 2005.

[4] Steinar Danielsen. *Electric Traction Power System Stability*. Norwegian University of Science and Technology, 2010.

[5] Thomas Høyvik Garten. *Linear Model of Rotary Converter in Traction Power System*. NTNU, 2006.

[6] B. L. Robertson I. A. Terry. *Single-Phase Synchronous Machine*. AIEE, 1947.

[7] James R. Bumby Jan Machowski, Janusz W. Bialek. Power system dynamics stability and control - second edition. 2008.

[8] Bjarne A. Foss Jens G. Balchen, Trond Andresen. *Reguleringsteknikk*. Institutt for teknisk kybernetikk, NTNU, 2003.

[9] Bengt Johansson. *2011021-11-2.0 Kompatibilitetsstudie för borstlös magnetisering*. Solvina AB, 2012.

[10] Emil Johansson. *Detailed Description of Synchronous Machine Models Used in Simpow*. Kungl Tekniska Högskolan, 2002.

[11] Ole Johan Ekeli Klingan. *Belastbarhet for roterende frekvensomformere for jernbanen i Norge*. NTNU, 2014.

[12] P. Kundur. *Power System Stability and Control*. McGraw-Hill, 1994.

[13] P.G. Murthy M. Pavella. *Transient Stability of Power Systems*. John Wiley Sons, 1994.

[14] T. A. Lipo R. J. Kerkman, P. C. Krause. *Simulation of a Synchronous Machine With an Open Phase*. 1977.

[15] IEEE Power Engineering Society. *IEEE Guide for Synchronous Generator Modeling Practices and Applications in Power System Stability Analyses*. The Institute of Electrical and Electronics Engineers, Inc, 2003.

[16] IEEE Power Engineering Society. *IEEE Recommended Practice for Calculating Short - Circ uit Currents in Industrial and Commercial Power Systems*. IEEE, 2006.

[17] IEEE Power Engineering Society. *IEEE Recommended Practice for Excitation System Models for Power System Stability Studies*. IEEE, 2006.

[18] Andreas Steimel. *Electric Traction - Motive Power and Energy Supply*. Oldenbourg Industrieverlag GmbH, 2008.

[19] Torsten Stoltze. *Dynamisches Verhalten von Synchron-Synchron-Umformern*. 1992.

[20] Magni T. Pálsson Trond Toftevaag. *LOW-FREQUENCY OSCILLATIONS IN THE NORWEGIAN ELECTRIC TRACTION POWER SUPPLY SYSTEM CAUSED BY INTERACTION BETWEEN THE SUPPLY SYSTEM AND PROPULSION MACHINERY – ANALYSIS AND CONSEQUENCES*. 7th International Conference “Modern Electric Traction in Integrated XXI st Century Europe”, 2005.

Appendix A

Equations of motion

The swing equation

The swing equation is a differential equation describing the dynamics of the machine rotor during the transient period. The rotor angle (measured with time) relative to the stator is the output of this equation. This is done by using fundamental mechanical laws, such as the Newton law:

$$T_{net} = J\alpha \tag{A.1}$$

The T_{net} stands for the net mechanical torque of the rotor, the J is the combined moment of inertia of all rotating parts.The α is the acceleration (or deceleration) of the rotor.

The acceleration is defined as

$$\alpha = \frac{d\omega_{mech}}{dt} = \frac{d^2\delta_m}{dt^2} \tag{A.2}$$

The δ_m is introduced here as the rotor angle measured with respect to a *synchronously rotating* reference frame:

$$\delta_m = \theta_m - (\omega_{m0}t + \theta_0) \tag{A.3}$$

The θ_m is the rotor angle measured with respect to the stationary reference frame, the ω_{m0} is the rated angular speed of the rotor. θ_0 is a constant equal to $\frac{pi}{2}$ since the q-axis lags the d-axis.

The kinetic energy stored in the rotor is:

$$E = \frac{1}{2} I \omega_{mech}^2 \tag{A.4}$$

Where ω_{mech} is the rotational speed of the rotor.

There are various torques acting on the rotor:

- The electromagnetic torque:
  - The synchronizing torque T_g: In phase with the rotor angle. Equal to the electrical output torque plus losses.
  - The damping torque T_{DD}: Produced by the equivalent electrical circuits due to asynchronous action. In phase with the rotor speed.
- Damping torques T_D: The sum of all damping in the system: generator controls, prime mover, power system and loads. Can be combined with T_{DD}. Proportional to rotor speed deviations.

  Can be decomposed: $T_D = D_d \frac{d\delta_m}{dt}$ where D_d is the damping parameter.
- Mechanical input torque T_m: The mechanical input on the rotor shaft from the prime mover. In the rotary converter, this is the torque produced by the three phase motor.

The net torque can now be defined as a sum of these torques :

$$T_{net} = T_m - T_g - T_D \tag{A.5}$$

With this stated, the swing equation can be formulated as:

$$J \frac{d^2 \delta_m}{dt^2} = T_m - T_g - T_D \tag{A.6}$$

(Where J is the moment inertia of inertia in the whole system given in kgm^2)

If one would like to express this by the means of the electrical angle (also known as the power angle), one can use the relation

$$\delta_e = \frac{p}{2}\delta_m \tag{A.7}$$

In most machine specifications, the inertia parameter is expressed by the inertia constant H. This is the combined constant of the whole system including prime mover, generator and exciter system. H is the stored kinetic energy at rated speed divided by the rated apparent power of the machine:

$$H = \frac{\frac{1}{2}J\omega_{m0}^2}{S_{B(3\phi)}} \tag{A.8}$$

The unit of H is seconds.

The swing equation is now rearranged in order to include the H constant and transforming all units to p.u.:

$$J = \frac{2HS_B}{\omega_{m0}^2} \tag{A.9}$$

$$\frac{d\Delta\omega_m}{dt} = \frac{1}{2H}(T_m - T_g - T_D) \tag{A.10}$$

Where $\Delta\omega_m = \frac{1}{\omega_{m0}}\frac{d\delta_m}{dt}$.

Appendix B

Parameter values

All the parameter values are fetched from [123].

B.1 Transformers

Table B.1: Parameter values of the transformers used in the model

Parameter		Motor side	Generator side	Unit
SN	Rated power	4.4	4.0	MVA
UN1	Rated voltage winding 1	66	4.0	kV
UN2	Rated voltage winding 2	6.3	16.6	kV
R	Short-circuit resistance	0.0054	0.014	pu
X	Short-circuit reactance	0.079	0.034	pu

B.2 Synchronous machines in the rotary converter

Table B.2: Parameter values of the synchronous machines in the rotary converter ASEA Q38

Parameter		Motor	Generator	Unit
SN	Rated power	4.4	4.0	MVA
UN	Rated voltage	6.3	4.0	kV
Xa	Stator leakage reactance	0.11	0.096	pu
Ra	Stator resistance	0.0033	0.00175	pu
Xd	D-axis synchronous reactance	0.90	1.02	pu
Xd'	D-axis transient reactance	0.24	0.12	pu
Xd"	D-axis sub-transient reactance	0.165	0.10	
Xq	Q-axis synchronous reactance	0.40	0.47	pu
Xq"	Q-axis sub-transient reactance	0.34	0.11	pu
Td0'	D-axis transient time constant	4.0	8.6	s
Td0"	D-axis sub-transient time constant	0.04	0.08	s
Tq0"	Q-axissub-transient time constant	0.10	3.4	s
H	Inertia constant	1.70	1.87	MWs/MVA

B.3 Line

The line at the single-phase side has the following impedance pr km:

$$Z_{line,km} = 0.17 + j0.20$$

This impedance is given in ohms/km.

B.4 AVR and exciter

Table B.3: The parameters of the DC1A voltage regulator

Parameter		Motor side	Generator side	Unit
Tr	Regulatorinput filter time constant	0.005	0.015	s
Ka	Regulator amplifier gain	382	382	pu
Ta	Regulator amplifier time constant	0.11	0.11	s
Ke	Exciter constant related to self-excited field	0.0	0.0	pu
Kf	Regulator stabiliser circuit gain	0.04	0.04	pu
Tf	Regulator stabiliser circuit time constant	0.7	0.7	s
VRmin	Min value of regulator output	-2.9	-3.5	pu
VRmax	Max value of regulator output	2.9	3.5	pu

Motstandsverdier ved 15° C

Omf. R103 nr.	Motor		Generator		Målt ved	Anm.
	Stator ohm	Rotor ohm	Stator ohm	Rotor ohm		
1	0,0854	0,332	0,01854	0,201	18,0	
2	0,0841	0,338	0,0184	0,202	17,4°	
3	0,0830	0,326	0,0178	0,199	18,1°	
4	0,0830	0,327	0,0182	0,201	18,8°	
5	0,0833	0,329	0,01815	0,199	18,0°	
6	0,0827	0,329	0,01815	0,202	19,3°	
7	0,0833	0,338	0,01795	0,203	19,0°	
8	0,0833	0,327	0,0179	0,200	20,0°	
9	0,0811	0,329	0,0179	0,201	17,8°	
10	0,0818	0,331	0,0178	0,199	16,5°	
11	0,0831	0,343	0,0183	0,213	20,0°	
12	0,0816	0,338	0,0181	0,198	17,6°	
13	0,0825	0,332	0,0182	0,198	18,1°	
14	0,0826	0,340	0,0182	0,204	19,0°	
15	0,0816	0,333	0,0180	0,203	20,0°	
16	0,0814	0,341	0,0183	0,205	21,0°	
17	0,0833	0,333	0,01812	0,2045	18,2°	
18	0,0826	0,352	0,01807	0,2005	19,0°	
19	0,0834	0,345	0,0180	0,201	17,5°	
20	0,0849	0,345	0,0181	0,203	20,3°	
21	0,0822	0,341	0,0177	0,202	18,7°	18,2° f. gen.
22	0,0831	0,341	0,0181	0,2093	20,6°	
23	0,0829	0,343	0,0180	0,205	20,5°	
24	0,0831	0,3355	0,0179	0,1997	20,0°	
25	0,0836	0,3510	0,0181	0,2057	21,2°	
26	0,0820	0,332	0,01765	0,1993	15°	
27	0,0830	0,332	0,01785	0,2015	"	
28	0,0818	0,327	0,01766	0,1985	"	
29	0,0825	0,343	0,01779	0,2010	"	
30	0,0828	0,329	0,01788	0,2025	"	
31	0,0810	0,327	0,01745	0,2000	"	
32	0,0807	0,328	0,01750	0,1990	"	

Appendix C

Drawing in HiDraw

The following is illustrating an attempt in building the model.

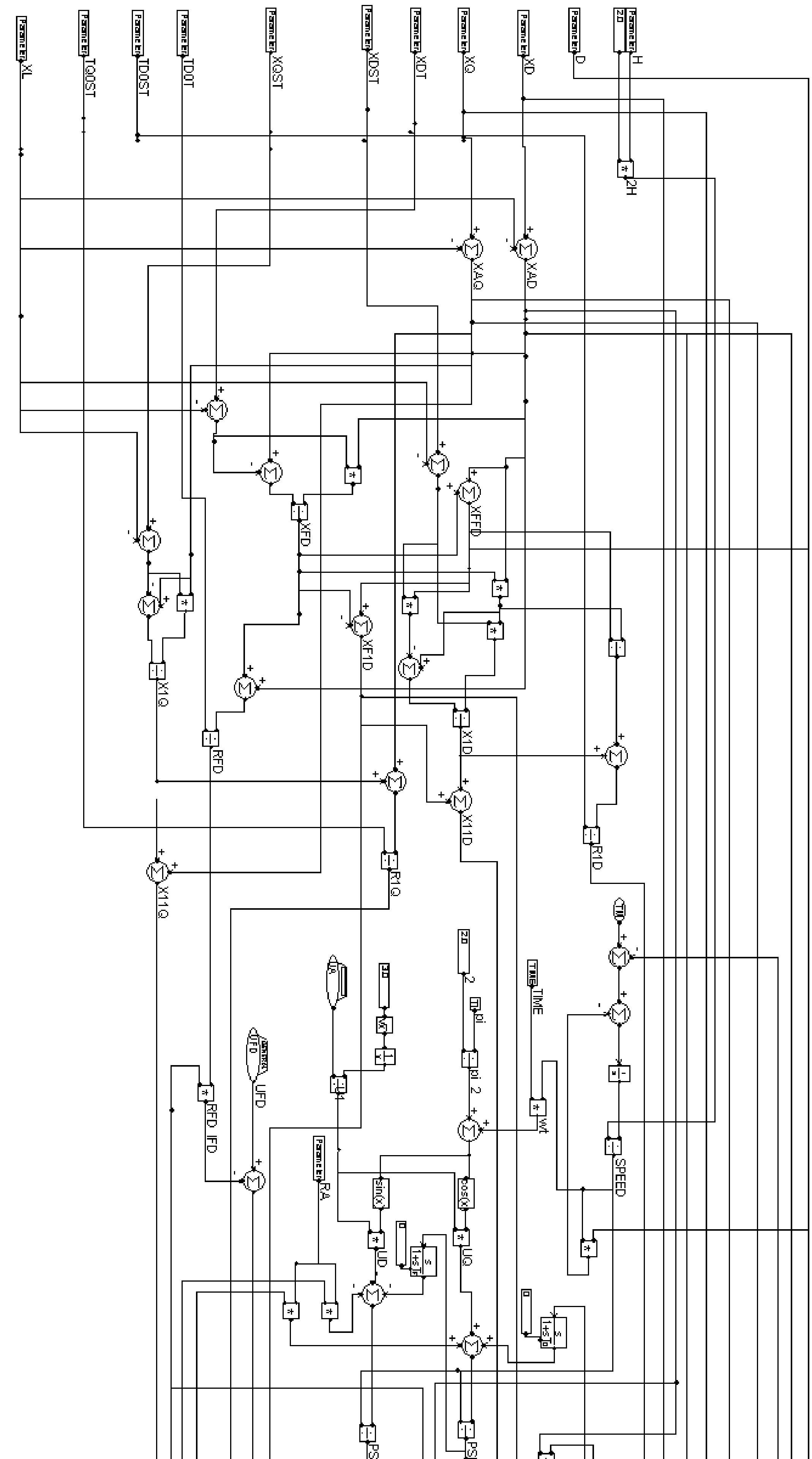
XL
TQ0ST
TD0ST
TD0T
XQST
XDST
XDT
XQ
XD
D
H
2H
XAQ
XAD
XFD
XFFD
XF1D
X1Q
RFD
X1D
X11D
R1Q
X11Q
R1D
TIME
SPEED
wt
UD
UQ
RA
UFD
RFD_IFD

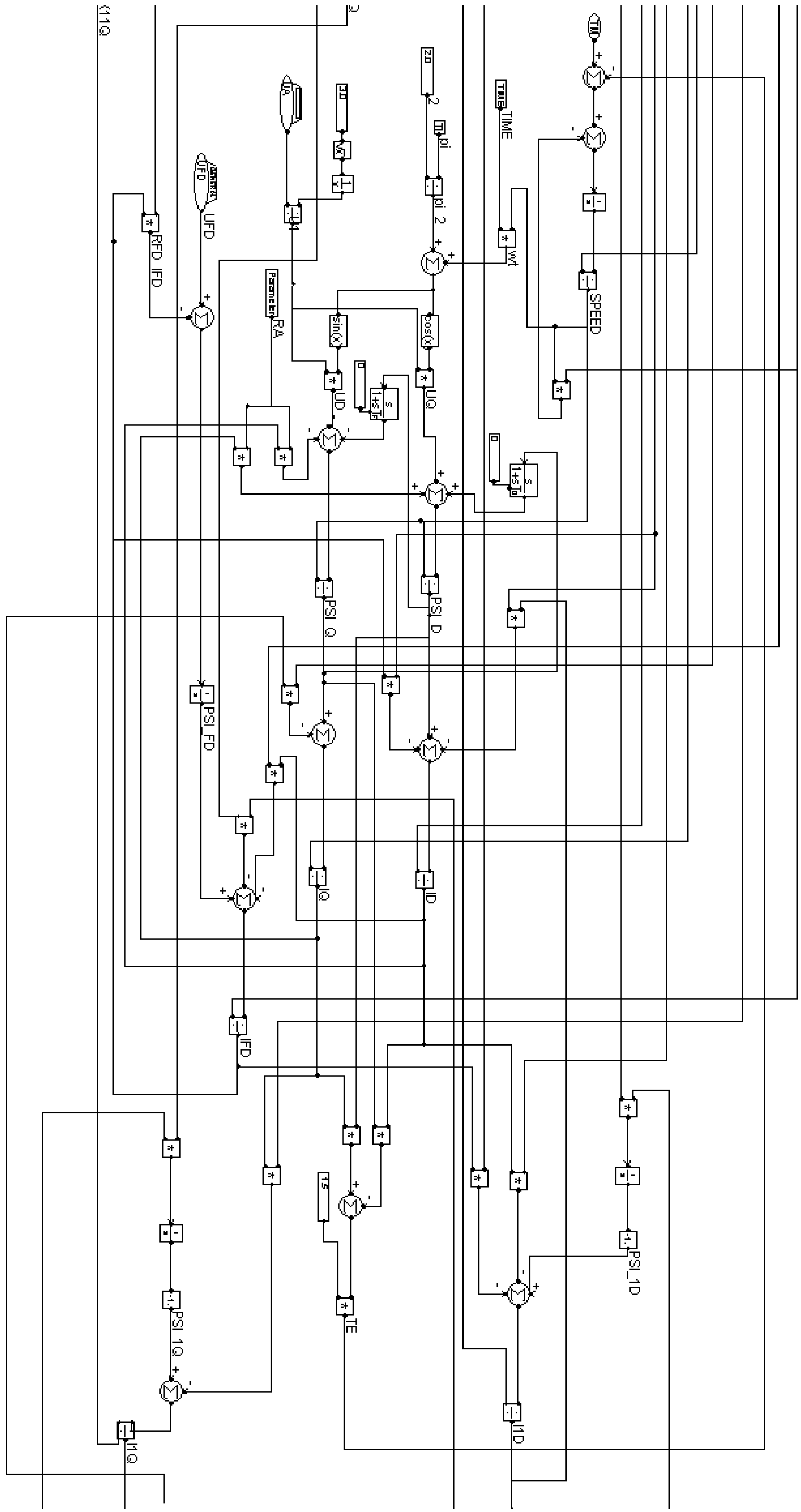
RFD IFD
UFD
RA
sin(x)
cos(x)
UD
UQ
TIME
wt
SPEED
PSI Q
PSI D
PSI_FD
IQ
ID
IFD
PSI 1Q
I1Q
TE
PSI_1D
I1D

Appendix D

DSL code

Here is the unfinished DSL-code for the model:

```
PROCESS TYPE2A(NODE1,SN,UN,H,D,RA,XD,XQ,XDP,
& XDB,XQB,XA,TD0P,TD0B,TQ0B,
& U0,FI0,P0,Q0,UF0,TET0,
& UF,VC,MECH0,MECH,SPEED,TETR,ICON,
& ISP,SPE,LDIDT)

EXTERNAL SN,UN,H,D,RA,XD,XQ,XDP
EXTERNAL XDB,XQB,XA,TD0B,TD0P,TQ0B
EXTERNAL U0,FI0,P0,Q0,UF
EXTERNAL MECH,TETR,ISP,SPE,LDIDT

INTEGER  ICON,ISP,SPE
REAL     VC,UF0/*/,MECH0/*/,TET0/*/,TETR,XQB,TQ0B,TM,LDIDT
REAL     U0,FI0/*/,P0,Q0,TD0B,XDB

REAL     HEIGHT,BASE,I0,TETAI,FI
REAL     SN,UN,H,D,RA,XA,XD,XQ,XDP,TD0P,UF,MECH
REAL     XAD/*/,XAQ/*/,XRF/*/,TF/*/,UB/*/,W0/*/
REAL     SIGMAFD/*/,TD/*/,XDD/*/,RF/*/
REAL     UBASE/*/,IBASE/*/,XQ1/*/,XQ2/*/,TQ1/*/,TQ2/*/
REAL     URE,UIM,SINT,COST,PSID,PSIQ,IF,RME,PSIDD,PSIQ1
```

```
REAL      IRE,IIM,UD,UQ,WD,WQ,FWD,FWQ
REAL      XFD,RFD,X1D,X1Q,R1D,R1Q,XFFD,XF1D,X11D,X11Q
REAL      TETA,SPEED,PSIF,ID,IQ,IDD,IQ1,UAA,UBB,UCC,KOEF
REAL      XFFD_INV, XD_INV, XQ_INV, SPEED_INV, X
REAL UDPLOT, UQPLOT, UOPLOT, UAPLOT, UBPLOT, UCPLOT
REAL FII0/*/, U1PLOT, I1PLOT
REAL U2, PX, QX, FAC1, FAC2
REAL UBX/*/, RIBASE/*/
REAL RIF, URMS
REAL RIRE, RIIM, UDL, UQL
REAL RID, RIQ, RIDG, RIQG, RI

STATE     TETA,SPEED,PSIF,ID,IQ,PSIDD,PSIQ1,IDD,IQ1,FI,TETAI
STATE     ICON/0/,PSID,PSIQ, X, RID, RIQ, URMS

AC        NODE1

REAL      I,P,Q,PD,PQ, URMSS
PLOT      SPEED,TETA, U1PLOT, RME, TM
PLOT     I1PLOT, UDL, UQL, SINT

XAD = XD - XA
XAQ = XQ - XA
XFD = XAD*(XDP - XA)/(XAD + XA - XDP)
RFD = (XAD + XFD)/TDOP
X1D = XAD*XFD*(XDB - XA)/(XAD*XFD - (XDB - XA)*(XAD + XFD))
X1Q = XAQ*(XQB - XA)/(XAQ + XA - XQB)
R1D = (X1D + XAD*XFD/(XAD + XFD))/TDOB
R1Q = (XAQ + X1Q)/TQOB
XFFD = XAD + XFD
XFFD_INV = 1/XFFD
XF1D = XFFD - XFD
X11D = X1D + XF1D
X11Q = X1Q + XAQ
TM = MECH
```

```
IF (START) THEN
        !U0=SQRT(UPRE(NODE1)*UPRE(NODE1)+UPIM(NODE1)*UPIM(NODE1))
        FII0=ATAN2(UPIM(NODE1),UPRE(NODE1))
        XRF=XAD*XAD/(XD-XDP)
        TF=TD0P
        UBX=UBASE(NODE1)/UN
        ... UBX is network voltage base value relative to rated motor
           voltage ...
        RIBASE=UBX*SN/SBASE
        ... RIBASE is rated motor current relative to network base current
            ...
        SPEED=1.
        FAC1=RA*RA+XQ*XQ
        U2=U0*U0
        PX=P0/U2
        QX=Q0/U2
        FAC2=1.+(PX*PX+QX*QX)*FAC1+2.*(PX*RA+QX*XQ)
        FAC2=SQRT(FAC2)
        !UDL=UBX*U0*(PX*XQ-QX*RA)/FAC2
        !UQL=UBX*U0*(1.+PX*RA+QX*XQ)/FAC2
        ... ATAN2(UDL,UQL) is the internal load angle ...


        !RID=PX*UDL+QX*UQL
        !RIQ=PX*UQL-QX*UDL

          IF(DISC.AND.(P0.EQ.0)) THEN
                       FI = PI/2
          ELSEIF(DISC.AND.(Q0.EQ.0)) THEN
                       FI = 0
          ELSE
                       FI = ATAN2(Q0,P0)
          ENDIF
          I0=SQRT(P0**2+Q0**2)/U0
           BASE=U0+RA*I0*COS(FI)+XQ*I0*SIN(FI)
      !opposite cathetus of fig. 3.23 (kundur)
```

```
      HEIGHT=XQ*I0*COS(FI)-RA*I0*SIN(FI)
      !internal load angle
      !!IF (DISC.AND.(BASE.NE.0.OR.HEIGHT.NE.0)) THEN
      TETAI=ATAN2(HEIGHT,BASE)
      !!ELSE
      !!   TETAI: BASE*SIN(TETAI)=HEIGHT*COS(TETAI)
      !!ENDIF

          RID=I0*SIN(TETAI+FI)*UBX
      RIQ=I0*COS(TETAI+FI)*UBX
          UDL=U0*SIN(TETAI)*UBX
      UQL=U0*COS(TETAI)*UBX
        TETA=ATAN2(UDL,UQL)+FII0
        PSID=UQL+RA*RIQ
        PSIQ=-(UDL+RA*RID)
        FWD=PSID+RID*XA
        FWQ=PSIQ+RIQ*XA
        WD=FWD
        WQ=FWQ
        !RIF=WD+RID*(XD-XA)
        RIF = UF/RFD
        FAC1=(XD-XDP)/(XD-XA)
        PSIF=RIF*(1.-FAC1)+FAC1*FWD

        URMS = U0
ENDIF


!RIF=(PSIF-(PSID+XA*RID)*XAD/XRF)/(1.-XAD/XRF)
RIF = (PSIF - XAD*RID - XF1D*RID)*XFFD_INV
RME=PSID*RIQ-PSIQ*RID


IF (TRANSTA) THEN
        URE=UPRE(NODE1)*UBX
        UIM=UPIM(NODE1)*UBX
```

```
        SINT=SIN(TETA)
        COST=COS(TETA)
        UDL=URE*SINT-UIM*COST
        UQL=URE*COST+UIM*SINT
        PSID: PSID=(UQL+RIQ*RA)/SPEED
        PSIQ: PSIQ=-(UDL+RID*RA)/SPEED
        RIRE=RID*SINT+RIQ*COST
        RIIM=RIQ*SINT-RID*COST
        IPRE(NODE1)=RIRE*RIBASE
        IPIM(NODE1)=RIIM*RIBASE
        I1PLOT = SQRT(RIRE**2 + RIIM**2)
        VC = SQRT(URE**2 + UIM**2)
        U1PLOT = VC

ELSE


        IF(ONE_PHASE(NODE1)) THEN
                        SINT=SIN(TETA+FI0-PI/2-FIREF)
                        COST=COS(TETA+FI0-PI/2-FIREF)
                        UDL=(UD(NODE1)*COST+UQ(NODE1)*SINT)*UBX
                        UQL=(UQ(NODE1)*COST-UD(NODE1)*SINT)*UBX
                        RIDG=RID*COST-RIQ*SINT
                        RIQG=RIQ*COST+RID*SINT
                        ID(NODE1)=RIDG*RIBASE
                        IQ(NODE1)=RIQG*RIBASE
                        I0(NODE1)=0.
                        W0 = .D/DT.FI0
                        !PSID: UDL+RID*RA+SPEED*PSIQ-.D/DT.PSID/.D/DT.FI0
                           =0.
                        PSIQ: PSIQ*SPEED = -(UDL + RA*RID + .D/DT.PSID)
                        X = PSID
                        !PSIQ: UQL+RIQ*RA-SPEED*PSID-.D/DT.PSIQ/.D/DT.FI0
                           =0.
                        PSID: PSID*SPEED = (UQL + RA*RIQ + .D/DT.PSIQ)
                        VC = SQRT(UDL**2 + UQL**2)
```

```
                        UDPLOT = UD(NODE1)
                        UQPLOT = UQ(NODE1)
                        UOPLOT = U0(NODE1)
                        U1PLOT = SQRT(3)*(UD(NODE1) + UQ(NODE1))

                        I1PLOT = RID


                        I1PLOT = SQRT(ID**2 + IQ**2)*SQRT(3)*0.5


            ELSE
                        SINT=SIN(TETA+FI0-pi/2-FIREF)
                        COST=COS(TETA+FI0-pi/2-FIREF)
                        UDL=(UD(NODE1)*COST+UQ(NODE1)*SINT)*UBX
                        UQL=(UQ(NODE1)*COST-UD(NODE1)*SINT)*UBX
                        RIDG=RID*COST-RIQ*SINT
                        RIQG=RIQ*COST+RID*SINT
                        ID(NODE1)=RIDG*RIBASE
                        IQ(NODE1)=RIQG*RIBASE
                        I0(NODE1)=0.
                        PSID: UDL+RID*RA+SPEED*PSIQ-.D/DT.PSID/.D/DT.FI0
                          =0.
                        PSIQ: UQL+RIQ*RA-SPEED*PSID-.D/DT.PSIQ/.D/DT.FI0
                          =0.
                        VC = SQRT(UDL**2 + UQL**2)

                        UDPLOT = UD(NODE1)
                        UQPLOT = UQ(NODE1)
                        UOPLOT = U0(NODE1)

                        U1PLOT = UA(NODE1)
                        I1PLOT = RID
                        URMSS = 1
```

```
        ENDIF
ENDIF




IF (.NOT.START) THEN
XD_INV = 1/XD
XQ_INV = 1/XQ
TETA: (SPEED-1.)*.D/DT.FI0(NODE1)-.D/DT.TETA=0.
SPEED: TM-RME-.D/DT.SPEED*2.*H-D*(SPEED -1)=0.

PSIF: RFD*RIF + .D/DT.PSIF*TF - UF = 0
!RID: PSID+(XA+XAD)*RID-RIF=0.
RID: RID = (RIF*XAD - PSID)*XD_INV
RIQ: RIQ = PSIQ*XQ_INV
ENDIF

RI=SQRT(RID*RID+RIQ*RIQ)
END
```